의학박사 학위논문

The generation of cardiosphere from adult heart and the implication of LPAR4+ cardiac progenitor cells for the treatment in ischemic heart disease

허혈성 심장질환 치료를 위한 심장유래 cardiosphere 와 LPA 수용체 4 + 심근전구세포의 영향에 관한 연구

2015 년 2 월

서울대학교 대학원

의과학과 의과학전공

이 호 재

A thesis of the Degree of Doctor of Philosophy

허혈성 심장질환 치료를 위한 심장유래 cardiosphere 와 LPA 수용체 4 + 심근전구세포의 영향에 관한 연구

The generation of cardiosphere from adult heart and the implication of LPAR4+ cardiac progenitor cells for the treatment in ischemic heart disease

February 2015

Major in Biomedical Sciences

The Department of Biomedical Sciences

Seoul National University Graduate School

Ho-Jae Lee

The generation of cardiosphere from adult heart and the implication of LPAR4+ cardiac progenitor cells for the treatment in ischemic heart disease

지도 교수 김 효 수

이 논문을 의학박사 학위논문으로 제출함
2014년 10월

서울대학교 대학원
의과학과 전공
이 호 재

이호재의 의학박사 학위논문을 인준함
2014년 12월

위 원 장 _____ (인)

부위원장 _____ (인)

위 원 _____ (인)

위 원 _____ (인)

위 원 _____ (인)

The generation of cardiosphere from adult heart and the implication of LPAR4+ cardiac progenitor cells for the treatment in ischemic heart disease

By
Ho-Jae Lee

A thesis submitted to the Department of Biomedical Sciences in partial fulfillment of the requirements for the Degree of Doctor of Philosophy in Biomedical Science at Seoul National University College of Medicine

December 2014

Approved by Thesis Committee:

Professor _____Chairman

Professor _____Vice chairman

Professor _____

Professor _____

Professor _____

ABSTRACT

Cardiac stem cells are found only in small numbers in the adult heart. As a strategy to overcome the limitation of insufficient cell numbers, cardiosphere-derived cells (CDCs) have been previously introduced. Since two-dimensional CDCs showed lower stemness than 3-dimensional form, re-creating sphere from attached CDCs could overcome such barrier. Nevertheless, repeated primary culture remains as technical huddle due to passage-dependent loss of stemness. Here, I proposed a method for stemness recovery by 3-dimensional culture, and an extension strategy for enriched number of phase-bright cells obtained from heart tissue by *ex vivo* culture.

To screen a specific marker of phase-bright cells, microarray data analysis was performed. *Lysophosphatidic acid receptor 4 (LPAR4)* was increased in most of phase-bright cells. A higher number of phase-bright cells were generated after treatment of 1μM LPA. Simultaneously, the expression of stemness related genes were increased together in a 3-dimensional form and by LPA treatment. The *LPAR4* expressed phase-bright cells

cultured in 3-dimension were then differentiated into cardiomyocytes. FACS analysis showed that the markers of cardiomyocyte, troponin-T and α-SA were more highly expressed than differentiation of CDC control group.

In conclusion, the acquired phase-bright cells with sufficient cell number and 3-dimensional form can be useful for differentiation into cardiomyocyte. The expression of LPAR4 in adult cardiac progenitors associates with the activation of cardiac progenitor cells for the differentiation into cardiomyocyte.

*Some of these works are published in Molecular Therapy. 2012 sep;20(9), Biomaterials. 2013 Jan;34(3), Biomaterials. 2013 Dec;34(38).

Keywords: cardiac progenitor cells, cardiospheres, cell therapy
Student number: 2008-22012

CONTENTS

LIST OF FIGURES AND TABLES

Chapter 1

Chapter 2

Chapter 3

LIST OF ABBREVIATIONS

CS: Cardiosphere

CDC: Cardiosphere derived cell

1st CS: primary cardiosphere

2nd CS: Secondary cardiosphere

2nd-H: Secondary cardiosphere hanging drop group

2nd-S: Secondary cardiosphere single cell group

PDL: poly-D-lysine

FN: Fibronectin

CEM: complete explant medium

CGM: cardiosphere growth medium

DMEM: Dulbecco's Modified Eagle Medium

FBS: fetal bovine serum

BMP2: Bone morphogenetic protein 2

TGF beta: Transforming growth factor beta

VEGF: vascular endothelial cell growth factor

EGF : Epidermal growth factor

bFGF: basic fibroblast growth factor

FS: Fractional Shortening

EF: Ejection Fraction

LVESD: Left ventricular end-systolic diameter

LVEDD: Left ventricular end-diastolic diameter

ALP: Alkaline phosphatase

i.p: intra peritoneal

LPA: Lysophosphatidic acid

LPC: Lysophosphatidyl choline

LPAR4: Lysophosphatidic acid Receptor 4

RA: Right atrium

LA: Left atrium

RV: Right ventricle

LV: Left ventricle

SEP: septum

APX: apex

mES: mouse Embryonic Stem

iPS: induced Pluripotent Stem

sh: short hairpin

GENERAL INTRODUCTION

Cell therapy is a promising strategy for repairing damaged heart(1). During the last decade there had been remarkable investigation for clinical applications of stem/progenitor cells(2). Various types of extra-cardiac cells, such as bone marrow cells, have been proposed(3). Although the delivery of heterogeneous bone marrow cells that do not require an *in vitro* culture process has been shown to be a safe method, the clinical results and hemodynamic improvements have been modest for the past 10 years(4). Patient-derived autologous cardiac progenitor cells were tested as another cell sources as bone marrow cells demonstrated that intracoronary infusion was effective for cardiac repair and scar reduction in recent phase 1 trials (5, 6). However, there are several barriers that should be overcome to apply these techniques for clinical trials: to acquire a sufficient number of cells for *in vivo* experiment (5). In recent studies, c-kit (+) or sca-1 (+) cardiac stem/progenitor cells and its side population cells showed possibility that post-natal hearts possess resident stem/progenitor cells which are already imprinted as cardiovascular fate(6-8). None the less, these cells are hard to

maintain with *in vitro* propagation method for transplantation while the generation of 3-dimensional form, cardiospheres are relatively simple and it is susceptible to gain their stemness potency (6). Nevertheless, repeated primary culture cannot be avoided due to loss of stemness as time goes. So it needs to acquire one of the closest stem cell to nature, phase-bright cells from *ex-vivo* culture.

To discover a marker of the phase-bright cell, microarray was performed. Among the set of genes obtained, I found Lysophosphatidic acid receptor 4 (LPAR4) was expressed in phase-bright cells. Identification of LPAR4 was reported first in 2003 as a fourth novel LPA receptor and expressing in the early developmental stages for heart in mice (9). In the while, it has not been demonstrated in adult stem cells. If the phase-bright cells expressing LPAR4 can be acquired with large amount, it would be desirable to research as cardiac stem cells.

In this dissertation, one of the adult cardiac stem cell named "secondary cardiosphere" which is repeated 3-dimensional culture and a new strategy for escalation of differentiation-potency using phase-bright cells are described in the next three chapters.

CHAPTER 1

Enhancing the potency of cardiac stem cells with secondary cardiosphere formation

INTRODUCTION

Cell-based therapies have been investigated experimentally and clinically in the contexts of regenerating or repairing damaged hearts(3). Over the past decade, various extra cardiac cells have been proposed as potential cell sources. Recent studies have raised the possibility that postnatal hearts possess resident stem/progenitor cells, which presumably are imprinted with cardiovascular fate as compared with extra cardiac cells(7). However, these cells are complicated to maintain when propagated *in vitro* for transplantation purposes. Accordingly, a stable and reproducible strategy is demanded to acquire optimal cell populations *in vitro* and to enhance cellular engraftment following transplantation *in vivo* to facilitate cell therapy (5). To meet these challenges, I investigated on the availability of repeated sphere formation to find out if it could enhance the multi potency of cardiac stem/progenitor cells – primary cardiosphere formation(6) → cardiosphere derived cells (CDC)(10) → finally, secondary cardiosphere formation (2nd CS) by three-dimensional culture. In this chapter, I studied whether these cell types would consequently improve cardiac function after transplantation.

MATERIALS AND METHODS

1. Animals

Below 6 week C57BL/6J mice, β-actin promoter-driven eGFP expressing mice, Oct4-promoter-driven GFP mice and E-selectin knockout mice were used for isolation of phase-bright cells which would be cardiospheres later(11). Above 8 week C57BL/6J, Balb/c background athymic nude mice were used for myocardial infarction model. All animal experiments were performed after receiving approval from the Institutional Animal Care and Use Committee (IACUC) at Seoul National University Hospital, Seoul, Korea.

2. Collection of human cardiac tissue

Less than 10mg (one or two pieces) of human right ventricular septal tissue was obtained by endomyocardial biopsy from heart transplant patients who had undergone the scheduled procedures for rejection surveillance. The tissue sampling was approved by the Institutional Review Board (IRB) at Seoul National University Hospital and written informed consents were obtained from all participants.

3. Cell isolation and culture methods for cardiospheres

Mice or human heart biopsy were minced with and digested up to 3 times with 0.2% trypsin-EDTA and 0.1% collagenase type Ⅳ for 5 minutes. The minced fragments were neutralized in 10% FBS contained medium for 10 minutes. The tissues were cultured on fibronectin (FN)-coated dishes with complete explant medium (CEM) (Iscove's Modified Dulbecco's Medium (IMDM), 20% FBS, 2 mM L-glutamine, 0.1 mM 2-mercaptoethanol and antibiotics) at 37℃ for 1 to 2 weeks to propagate phase-bright cells. To generate primary cardiosphere(6), phase-bright cells were cultured on poly-D-lysine (PDL) coated dishes (BD) in cardiosphere growth medium (CGM)(35% IMDM, 65% DMEM-Ham F-12, 3.5% FBS, 2% B27, 25 ng/ml epidermal growth factor, 40 ng/ml basic fibroblast growth factor, 4 ng/ml cardiotropin-1, 1 unit thrombin, 2mM L-glutamine, 0.1 mM 2-mercaptoethanol and antibiotics). The 3 to 7days primary CSs were cultured on 0.124mg/ml fibronectin (FN)-coated dishes with cardiosphere growth media to generate cardiosphere-derived cells (CDCs)(10). Following trypsinization, CDCs were grown in a hanging-drop culture (12, 13), PDL dish, petridish and

Aggrewell^{TM} for 24 – 48hrs to generate secondary cardiospheres with CGM.

4. *In vitro* differentiation

Preparation of lineage tracing vectors: To assess *in vitro* differentiation potentials, I applied lineage tracing lentiviral vectors containing the eGFP gene before initiating differentiation (14, 15). The eGFP expression was controlled using eNOS promoter, VEGFR2 promoter for vessel endothelial cellular lineage, or α-myosin heavy chain promoter for cardiac muscle cellular lineage tracing. To perform the transduction of the lentivirus into CDCs, cells were incubated in CGM containing lentiviral particle for 24 hours. After 3 washes and a medium change, CDCs were subjected to differentiation assays (16).

Endothelial differentiation: Secondary cardiospheres were cultured on typed Ⅳ collagen-coated dishes and cultured in endothelial growth media (EGM2-MV, Lonza) contacting 5% FBS and additional VEGF (50 ng/ml) for 7 days. Endothelial differentiation was assessed by monitoring eGFP fluorescence from lineage tracing vectors, isolectin B4 staining.

Cardiomyogenic differentiation: Cells were plated on 1.5% gelatin-coated dishes and co-cultured with neonatal rat cardiomyocytes in differentiation media (DMEM/F12, 20% FBS, 10 ng/ml BMP2 and 10 ng/ml TGF-β)(17, 18).

5. Myocardial infarction induction and cell transplantation

Mice were anesthetized with Zoletil® (91 mg/kg, Virbac, i.p) and Xylazine® (11.65 mg/kg, Bayer, i.p), intubated and artificially ventilated (Harvard Apparatus). Through left-sided thoracotomy, the heart was exposed and the left anterior descending artery was ligated using 8-0 polypropylene sutures and a dissecting microscope. $1x10^5$ cells in 50μl of PBS were directly transplanted into peri-infarct areas and the apex (total 3 sites) using a 31G needle(19).

6. Physiologic assessments and histologic measurements

Two to three weeks after inducing myocardial infarction, LV functions were evaluated by echocardiography using 15.0-MHz ultraband linear transducer (Aplio XG, Toshiba, Japan). LV dimensions at end systole (LVESD) and end diastole (LVEDD) were measured. Fractional shortening, ejection fraction were

also calculated (19). After an echocardiographic examination, hearts were perfused retrogradely through the right carotid artery with PBS containing 4 % paraformaldehyde (PFA). Tissue were embedded in OCT compound (Sakura Finetek) or paraffin. Tissue sections were stained with Masson's trichrome staining (Sigma Aldrich) to measure infarct sizes. Percentage of fibrosis length and infarct thickness was measured using Image J software.

7. Immunostaining

Cells or tissue sections were incubated with antibodies against GFP (Abcam), Oct4 (Santa Cruz), c-kit (BD), Connexin 43 (Santa Cruz), Troponin T (Santa Cruz) and Nkx2.5 (Abcam). DAPI was used for nuclear counterstaining. To identify capillaries, isolectin B4 (Vector Laboratories) was used.

8. Flow cytometry

Single-dissociated human CDCs were incubated with the following fluorescence-labeled monoclonal antibodies: CD34 (AbD Serotec), CD44 (eBioscience), CD45 (DAKO), CD105 (AbD Serotec) and c-kit (eBioscience). An IgG isotype was

used to define the percentage of positive cells. Analyses were performed using FACS Aria™ (Becton Dickinson).

9. Statistical analysis

All data were expressed as means S.E.M. The student's t-test or one-way ANOVA with Bonferroni's correction were used for intergroup. SPSS version 12.0 was used throughout. A *P* value less than 0.05 denoted the presence of a statistically significant difference.

RESULTS

Generation of mice cardiospheres and cardiosphere-derived cells from explant culture

Cardiosphere was generated as flowing method (Figure 1-1A). To compare the cellular potencies of primary cardiosphere and CDC, I performed real-time PCR. The PCR data revealed that CDC has weaker gene expression of *Oct4, c-kit* than primary cardiosphere (Figure 1-1B). Alkaline phosphatase (ALP) and immunofluorescence (IF) staining showed consistent results with gene expression patterns (Figure 1-1C). I generated cardiosphere from Oct4 promoter-driven eGFP mice and confirmed that primary cardiosphere have strong eGFP signal but CDC was less (Figure 1-1C). The primary cardiosphere was bigger after time passed as gathering each other and fusion, but could not be increased in cell numbers as cell cycle. Primary CS had insufficient cell number for *in vivo* transplantation. Taken together, a primary cardiosphere possesses multipotency, but it may be hard to handle with regular size for the study. Moreover, the CDC, expanded by two-dimensional monolayer culture, has limited cellular potency.

Characteristics and differentiation potentials of secondary CSs

To overcome the limitations of monolayer culture, I investigated a repeated sphere formation strategy for enhancing the cellular potency. Spheres were generated from CDC using hanging-drop method, which is widely used for embryonic stem cell experiments to regulate cell numbers in spheres (12, 13). I hung 1,000 cells in a drop and 48 hours later observed uniformly-sized spheres (150 - 200 μm). I refer to the subsequently formed CS form CDC as "secondary cardiosphere". Compare to CDC, secondary CS recovered Oct4 and c-kit expression (Figure 1-2A). Next, I evaluated the differentiation potentials of secondary CS. First, I checked endothelial differentiation (Figure 2B, Left panel). Endothelial nitric oxide synthase (eNOS) promoter-driven eGFP reporter was transduced into CDC, and then secondary CS was generated and subsequently attached to dishes for differentiation. At the baseline before the induction of differentiation, there was no eGFP signal. After 7 days, a few CDC was found to express eGFP (2.7±0.7%). In contrast, many cells sprouted from secondary CS and expressed eGFP(16.3±4.2%, P = 0.02 compared with CDC, N = 4, each group). I performed the same

experiment by vascular endothelial growth factor receptor 2 (VEGFR2) promoter-driven eGFP reporters. Furthermore, these cells were positive for isolectin B4 (ILB4), a marker of endothelial cells. These findings indicate that secondary CS has greater endothelial differentiation potential than CDC has.

Second, I induced cardiomyogenic differentiation (Figure 1-2B, Right panel). CDCs and secondary CSs were co-cultured with rat cardiomyocytes. After 5 to 7 days, cells sprouted from secondary CSs and showed beating. Furthermore, connexin 43 (Cx43) was expressed between secondary CS and rat cardiomyocyte while CDC rarely contracted and few cells expressed Cx43. In another set of experiments, I transduced alpha myosin heavy chain (α-MHC) promoter-driven eGFP to monitor cardiomyocyte-specific gene expression. I observed α-MHC promoter was activated in the secondary CSs.

Secondary cardiosphere transplantation following myocardial infarction promotes cardiac repair

To investigate the functional benefits of cell transplantation into ischemic myocardium, I injected CDCs ($1x10^5$), secondary CSs ($1x10^5$) or PBS after left anterior descending artery ligation.

Regarding secondary CSs, I created two groups: the secondary cardiosphere-single cell dissociated group (the 2nd-S group) and the secondary cardiosphere-hanging drop group (the 2nd-H group). To produce secondary CSs with a consistent size, I generated secondary CSs containing 1,000 cells using the hanging-drop method prior to transplantation. In the 2nd-H group, 100 secondary cardiospheres were generated from $1x10^5$ CDCs by hanging-drop for 48 hours. In the single cell (2nd-S) group, secondary CSs were dissociated into single cells using trypsin. An echocardiographic examination at 14 days after transplantation showed that LV systolic function indices, such as, fractional shortening and ejection fraction (19), were better in groups treated with either one of 3 types cell transplantation (CDC, 2nd-S and 2nd-H groups) than with PBS (Figure 1-3A). In the short-term follow-up, there was no significant difference of global systolic function (FS and EF) between cell injection groups. However, importantly, in terms of LV remodeling, sphere transplantation (2nd-H group) was more effective than dissociated-single cell transplantation (2nd-S group) or CDCs in preventing LV dilatation of systolic and diastolic phases (P-value < 0.05, 2nd-H group versus CDC

and 2nd-S groups). These data suggest that the transplantation of secondary CSs in spherical form promotes cardiac repair and ameliorates adverse cardiac remodeling as compared with the transplantation of single-dissociated cells from secondary CSs or CDCs. To examine pathologic changes after MI and cell transplantation, I checked fibrosis lengths and infarct thicknesses (Figure 1-3B). Masson's trichrome staining revealed that secondary CS transplantation significantly reduced infarct size and increased wall thickness in infarcted areas, indicating the preservation or regeneration of functional myocardium.

Cardiomyogenic and vasculogenic differentiation of secondary cardiosphere *in vivo*

To evaluate the fate of engrafted cells at 7 and 14 days, I performed immune fluorescence staining with Nkx2.5 and Troponin T. In the group transplanted with spheres of secondary CS (2nd-H), transplanted cells found in the peri-infarct zone expressed Nkx2.5 at 7 days. But in the animals transplanted with CDCs or single-dissociated cells from secondary CS (2nd-S), the injected cells rarely expressed

Nkx2.5 (Figure 1-3C). Interestingly, some Nkx2.5-expressing cells did not express GFP, which suggested that they were resident cardiac cells rather than transplanted ones. These findings suggest that exogenous secondary CS transplantation may also activate endogenous cardiac stem/progenitor cells to differentiate into cardiomyocytes. I confirmed cardiomyogenic differentiation by immune fluorescence staining using antibodies against structural protein of cardiomyocytes, alpha sarcomeric actinin (α-SA) and GFP (Figure 3D, Upper panel). I also found that some GFP (+) cells formed capillary-like structures and they were positive for isolectin B4 (ILB4) (Figure 1-3D, Lower panel). These findings indicate that transplanted secondary CSs underwent cardiomyogenic and vasculogenic differentiation. These findings suggest that secondary CS-mediated neovascularization significantly contributes to functional improvements after MI and cell transplantation.

Generation of adult human secondary cardiospheres

I obtained one or two pieces (less than 10 mg) from right ventricular septal tissues by endomyocardial biopsy. The method for a generation of human secondary cardiosphere is

similar with mice secondary cardiosphere, but it needed more time (Figure 1-4A). First, at fifteen days after culturing the cardiac explant on fibronectin (FN)-coated dishes, I could observe phase-bright cells. To generate primary CSs, phase-bright cells were collected at day 21 using trypsin and reseeded on poly-D-lysine (PDL)-coated dishes. On day 24, approximately 100 primary CSs were obtained. These floating primary CSs were transferred and plated on FN-coated dishes and grew as adherent cells with a mesenchymal stromal cell-like (or fibroblast-like) morphology. Flow cytometry analysis was performed to characterize these human CDCs (Figure 1-4B). The majority of adherent cells expressed the mesenchymal lineage markers CD44 and CD105, but less than 1% expressed the hematopoietic cell-related marker CD45. A small proportion of cells expressed c-kit and CD34. Secondary CSs were generated from using the culture of CDCs again on poly-D-lysine (PDL)-coated dishes or using the hanging-drop suspension technique to escalate the cellular potency (13) which resulted in spheres that were uniform in size.

Comparison of methods to generate secondary cardiosphere

Variations in the size and number of cells in each sphere may significantly affect the gene expression profiles and alter the characteristics of the final product. In order to establish the best protocol for secondary CSs, I compared four different methods to generate secondary CSs; (1) Poly-D-lysine (PDL)-coated dishes, (2) Petri dishes, (3) the hanging-drop method, (4) AggreWell™ plates (Table 1-1). The morphology of the cells and spheres are shown in Figure 1-5A. The number, size and shape of the secondary CSs generated on poly-D-lysine (PDL)-coated dishes or Petri dishes were variable and unpredictable (50 - 200 μm). Several of the spheres aggregated together and formed irregularly-sized spheres. It took 72 hours for these methods to result in mature secondary CSs. In contrast, the secondary CSs generated using AggreWell™ plates or the hanging-drop method were homogenous in size and completely spherical and required a shorter period of time for maturation (approximately 3-24 hours and 12-48 hours, respectively). Spheres of uniform shape and size are important for generating the reproducible results from *in vitro* and *in vivo* experiments. The shortened time for cell processing is pivotal in clinical applications.

Furthermore, the mRNA expression of Oct4 or Nanog was more elevated when secondary CSs formed on the AggreWell™ plate or in hanging-drop cultures than when those on the poly-D-lysine (PDL)-coated dish or Petri dish (Figure 1-5B). Taken these data together, I found that the hanging-drop or AggreWell™ method was superior to the other method based on PDL-coated dish or Petri dish, in terms of the homogeneity of the final product, cellular potency and simplicity of the techniques. However, there are also drawbacks to both methods, including the high cost of the AggreWell™ plates and the requirement of intensive labor in hanging-drop procedure.

Differences in stemness between human CDC and secondary CS

The human CDCs were weakly positive following alkaline phosphatase (ALP) staining (Figure 1-6A). The intensity of ALP staining gradually increased after initiation of sphere formation. The human secondary CSs were strongly positive for ALP after 72 hours, which suggests that sphere formation may escalate the stemness of the cells. To confirm this finding, I examined the serial expression patterns of Oct4 using real-time PCR (Figure 1-6B, Left panel). The expression of Oct4

protein increased with sphere formation as determined by immunocytochemistry and confocal microscopic exam (Figure 1-6B, Right panel).

Transplantation of human secondary CSs into infarcted myocardium of nude mice

The ability of human secondary CS was assessed to differentiate into cardiovascular lineages *in vivo*. Myocardial infarction (20) was induced by the ligation of the left anterior descending artery in athymic nude mice, and then total $3x10^5$ cells (300 cells per sphere, with a total of 1000 secondary CSs) were transplanted into the peri-infarct sites. To determine the fate of transplanted cells, an eGFP lentiviral vector was transduced into secondary CSs prior to transplantation. After 2 weeks, the immunofluorescence staining revealed that the GFP (+) cells at the peri-infarct sites were elongated and striated and also expressed alpha sarcomeric actinin (α-SA) (Figure 1-7A). There were other GFP (+) cells that expressed VE-cadherin, a specific marker of endothelial cells (Figure 1-7B). These results suggest transplanted human secondary CSs can differentiate into cardiomyocytes and endothelial cells *in vivo*.

A

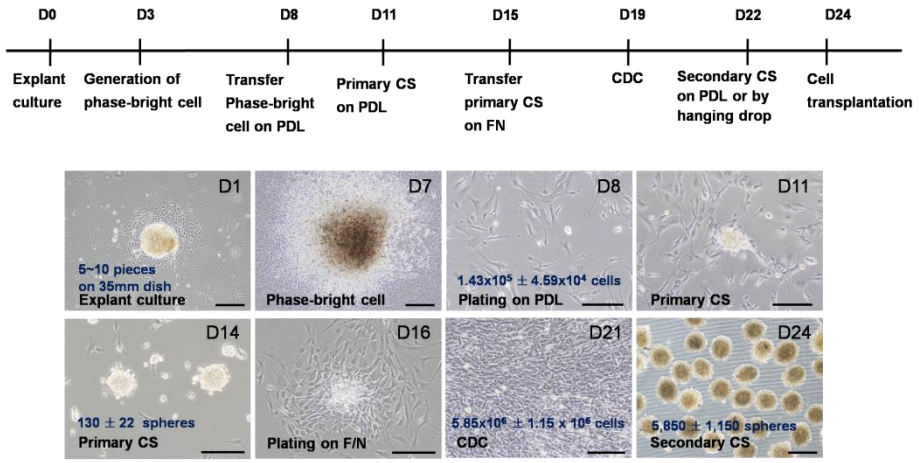

B

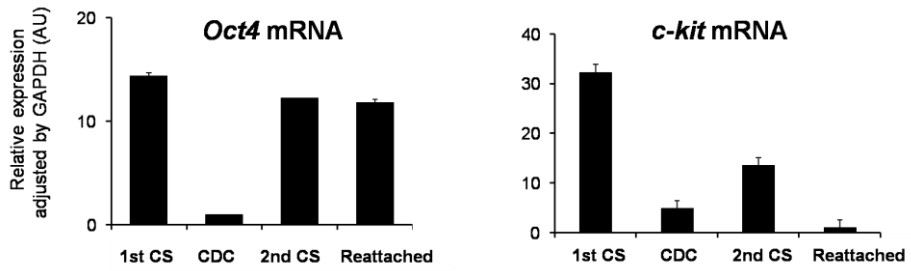

Figure 1-1 Generation of primary and secondary cardiospheres and their characteristics

(A) Timeline of primary CS, CDC, and secondary CS generation with average cell numbers (n = 5). Bar: 500 μm.

(B) The gene expressions of *Oct4* and *c-kit* were measured by real-time PCR.

C

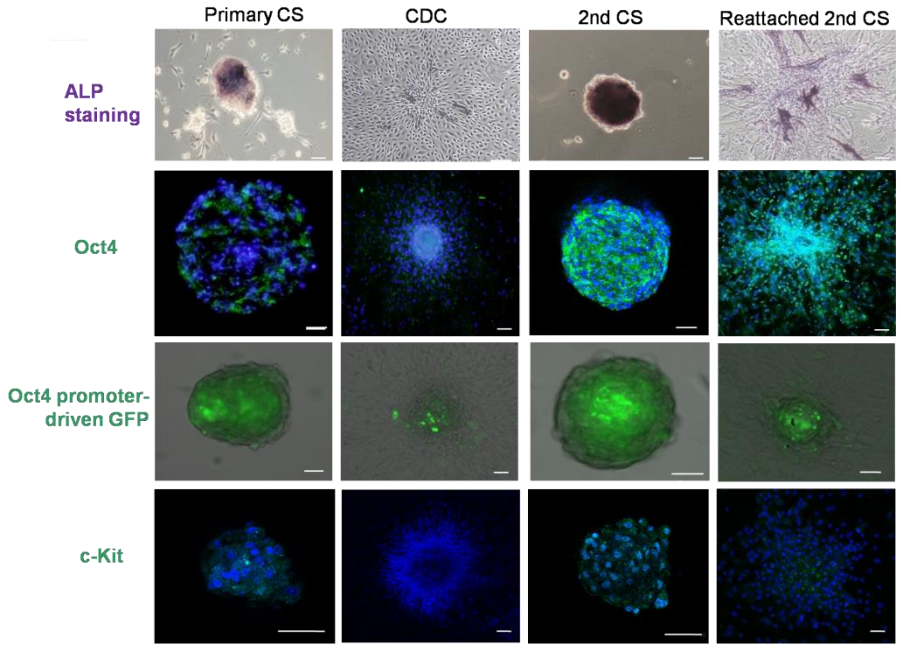

(C) Primary and secondary CSs were positive for alkaline phosphatase (ALP) staining, but CDCs were not.

The protein expressions of Oct4 and c-kit were assessed by confocal imaging. Oct4 expression was verified using Oct4 promoter-driven GFP cells. Secondary CSs expressed Oct4 and c-kit more homogeneously and densely than primary CSs, whereas CDCs lacked expressions. Bar: 50 μm.

A

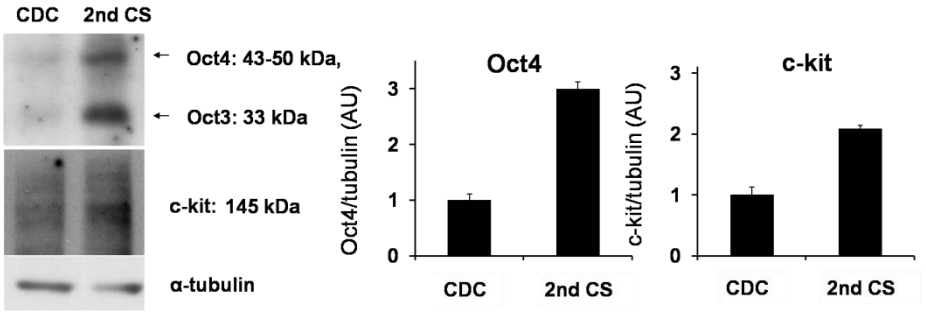

B

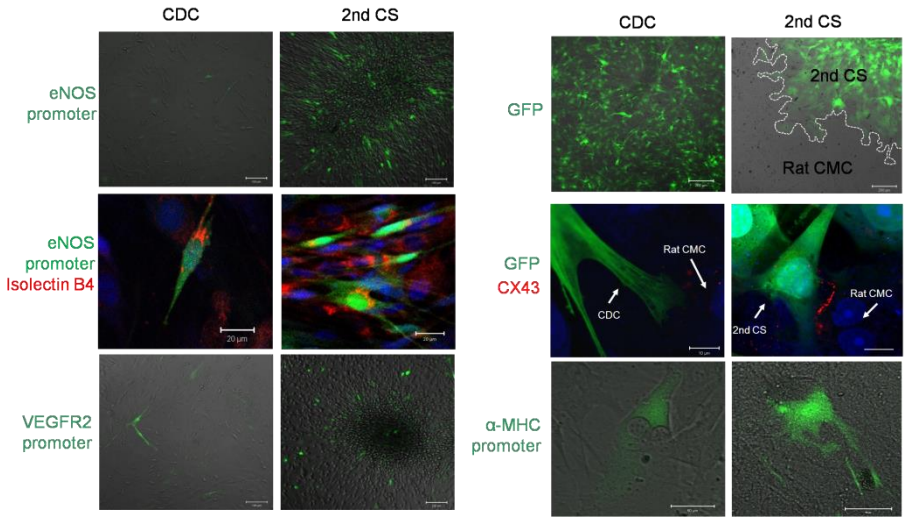

Figure 1-2 Stemness and Differentiation potentials of secondary cardiospheres

(A) The protein expressions of Oct4 and c-kit were measured by western blots and quantified by densitometry.

(B) Cells were transduced with eNOS promoter-driven eGFP or VEGFR2 promoter-driven eGFP using lentivirus. Seven days after differentiation induction, secondary CSs expressed GFP

but CDCs scarcely expressed. GFP-expressing cells were confirmed to have differentiated into the endothelial lineage by isolectin B4 staining. Cardiomyogenic differentiation was induced by co-culture with rat cardiomyocytes. Cells were from the heart of a β-actin promoter-driven eGFP-expressing mouse to distinguish them from rat cardiomyocytes or transduced with α-MHC promoter-driven eGFP reporter to validate cardiac differentiation. Cx43 was densely expressed between secondary CSs and rat cardiomyocytes. Bar: 50 μm.

A

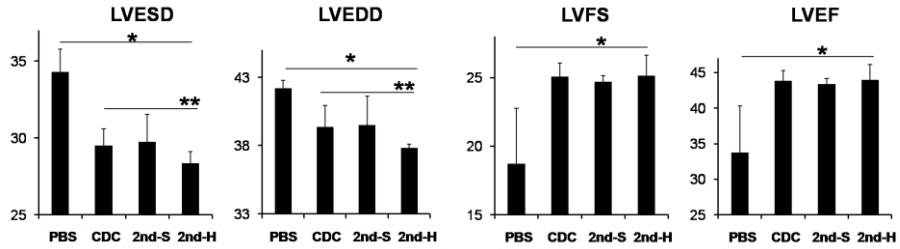
LVESD
LVEDD
LVFS
LVEF
PBS
CDC
2nd-S
2nd-H

B

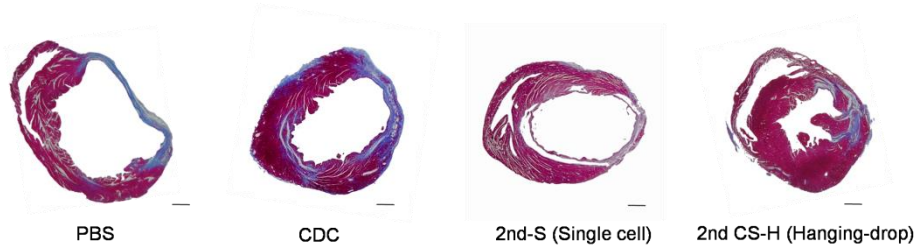
PBS
CDC
2nd-S (Single cell)
2nd CS-H (Hanging-drop)

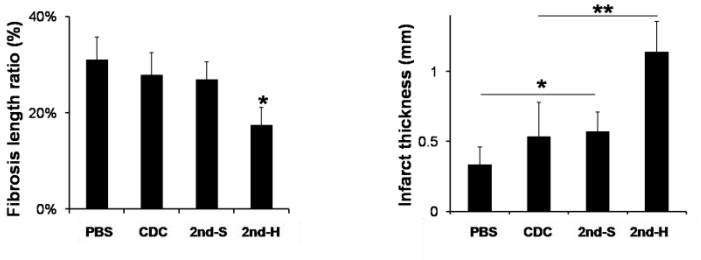
Fibrosis length ratio (%)
Infarct thickness (mm)
PBS
CDC
2nd-S
2nd-H

C

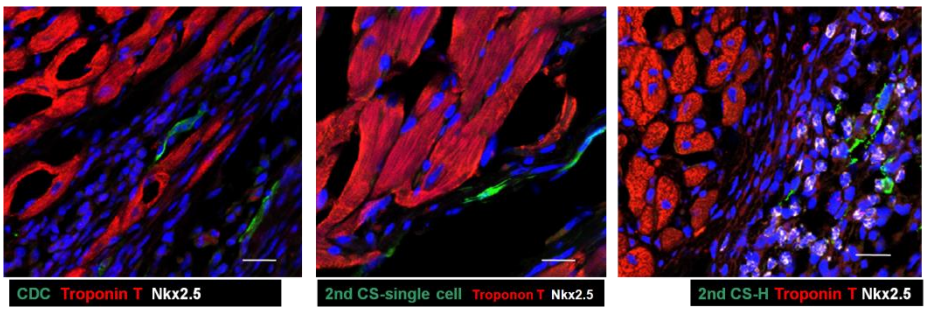
CDC Troponin T Nkx2.5
2nd CS-single cell Troponon T Nkx2.5
2nd CS-H Troponin T Nkx2.5

D

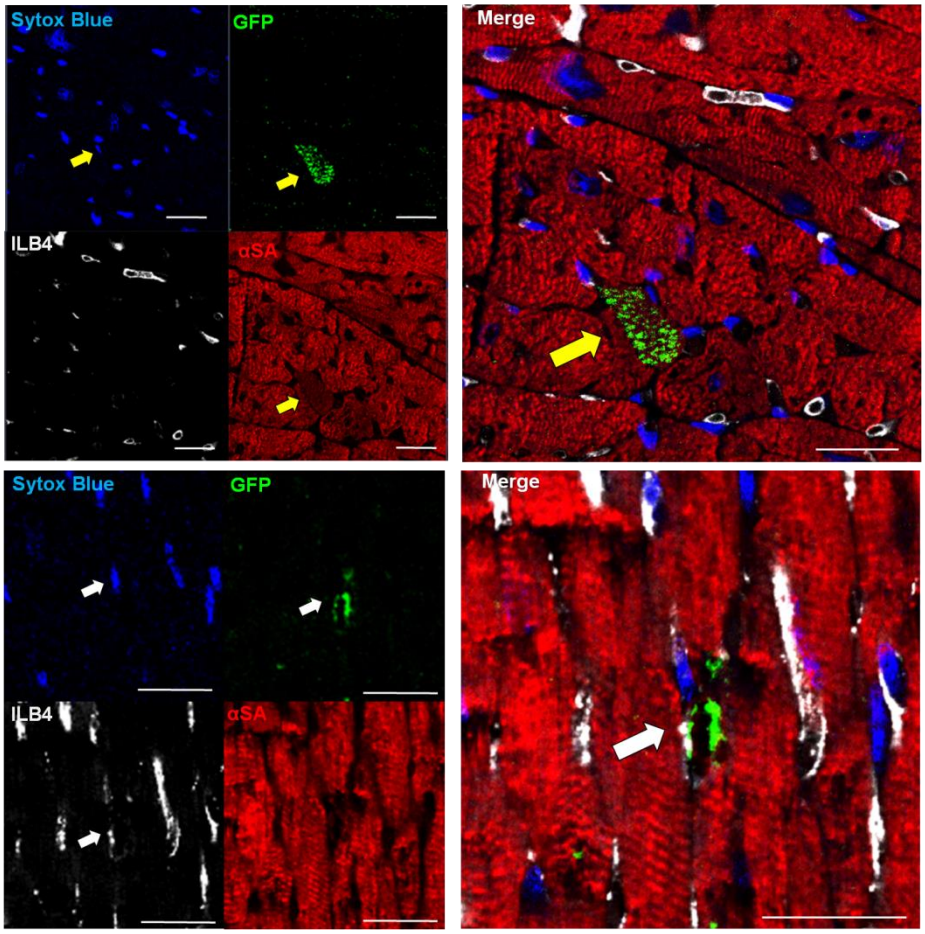

Figure 1-3 Transplantation of secondary cardiospheres into ischemic myocardium

(A) Echocardiographic parameters at 14 days after cell transplantation (n =6 per group, *P < 0.01, PBS versus the two transplanted groups; **P < 0.05, 2nd-H group versus CDC and 2nd-S groups).

(B) Masson's trichrome staining; 2nd-H transplantation markedly reduced infarct-related fibrosis length (*P < 0.01,

2nd-H group versus the other three groups). 2nd-H transplantation increased infarct thickness more than transplantation with CDCs or 2nd-S (*P < 0.05, PBS versus the CDC and 2nd-S groups; **P < 0.01, the 2nd-H group versus the CDC and 2nd-S groups). Bar: 500 μm.

(C) In the peri-infarct area at day 7 post-transplantation, engrafted CDCs and 2nd-S cells did not express cardiac transcription factor Nkx2.5. However, 2nd-H cells expressed Nkx2.5, and some Nkx2.5 (+) cells did not express GFP, suggesting that 2nd-H cells activated endogenous cardiac progenitor cells. Bar: 20 μm.

(D) At day 14, transplanted GFP (+) secondary CSs differentiated into the cardiomyocyte (yellow arrow) and the endothelial cell (white arrow). Bar: 20 μm.

A

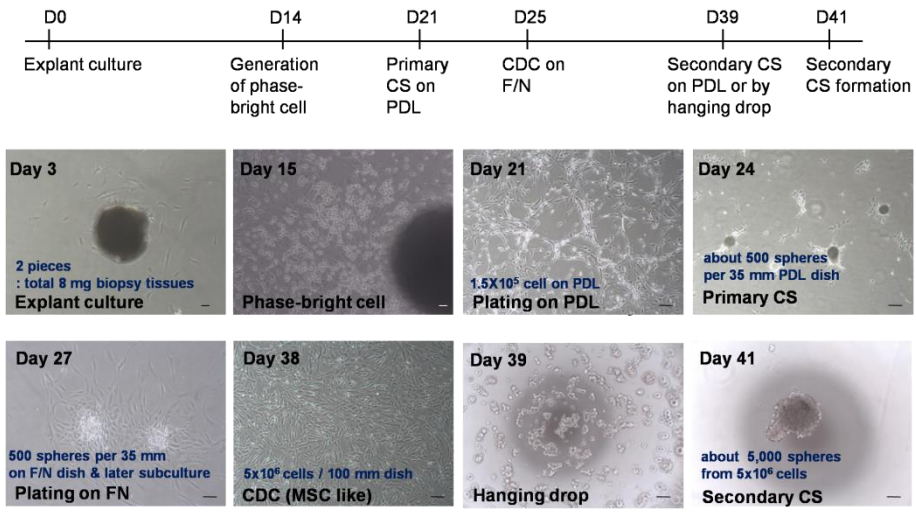

B

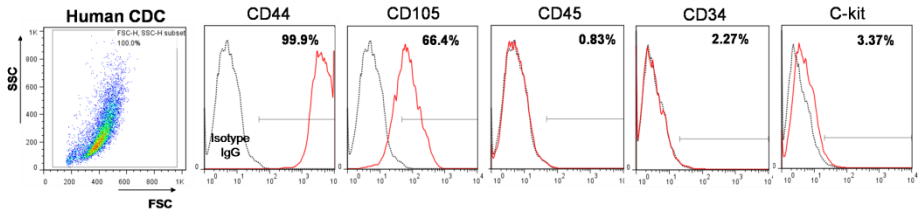

Figure 1-4 Generation of adult human secondary cardiosphere

(A) Timeline of human cardiac tissue processing to generate secondary CSs. Bar: 100 μm.

(B) FACS analysis showed that the majority of CDCs expressed CD44 and CD105, but did not express the hematopoietic cell-related marker CD45. Several cells expressed CD34 and c-kit.

A

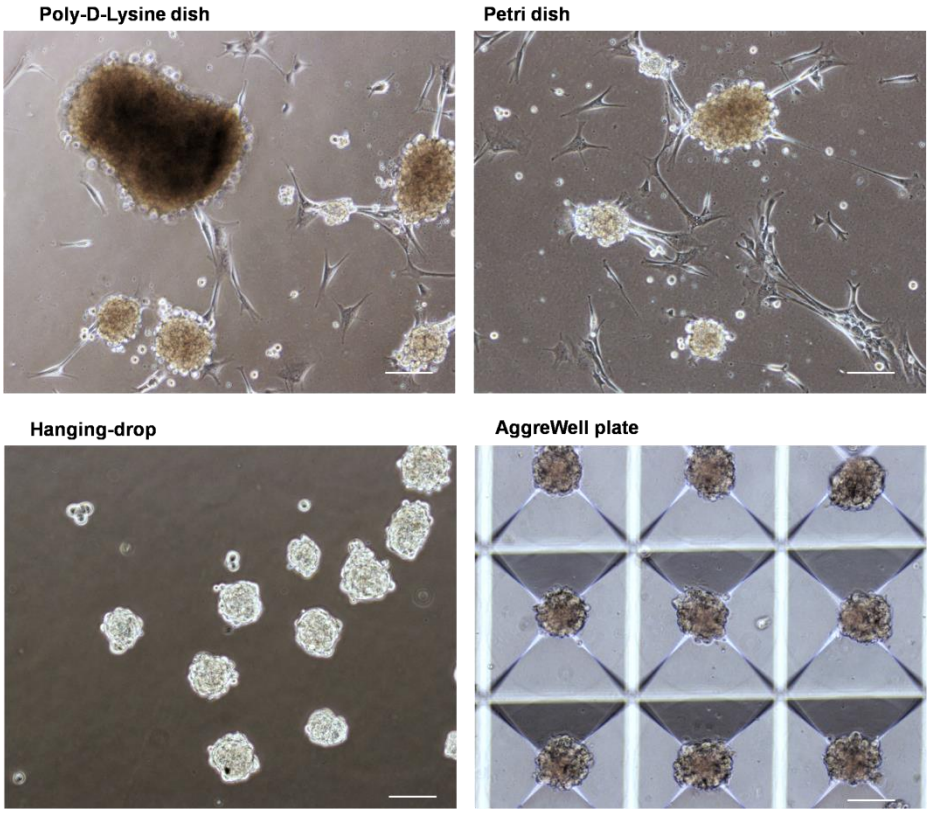
Poly-D-Lysine dish
Petri dish
Hanging-drop
AggreWell plate

B

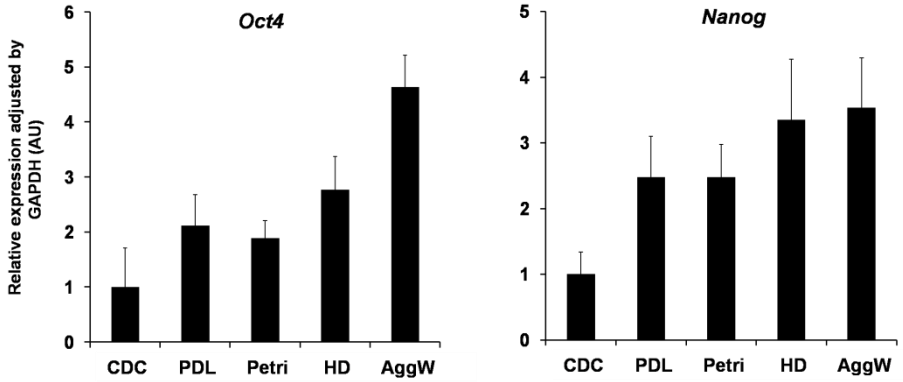
Oct4
Nanog
Relative expression adjusted by GAPDH (AU)
0
1
2
3
4
5
6
CDC
PDL
Petri
HD
AggW

Figure 1-5 Methods of generating secondary cardiospheres

(A) The morphology of the cells and spheres. The secondary CSs produced from AggreWell™ plates or the hanging-drop method was homogenous.

(B) The mRNA expression of Oct4 and Nanog were increased when secondary CSs were formed using the AggreWell™ plate or the hanging drop method compared to CSs grown on PDL-coated or Petri dishes (PDL, poly-D-lysine-coated dish; Petri, Petri dish; HD, hanging-drop; AggW, AggreWell plate™).

A

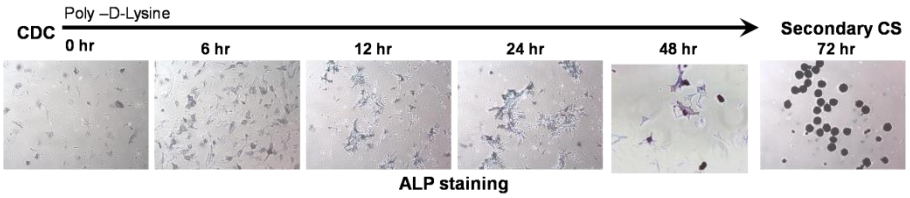

B

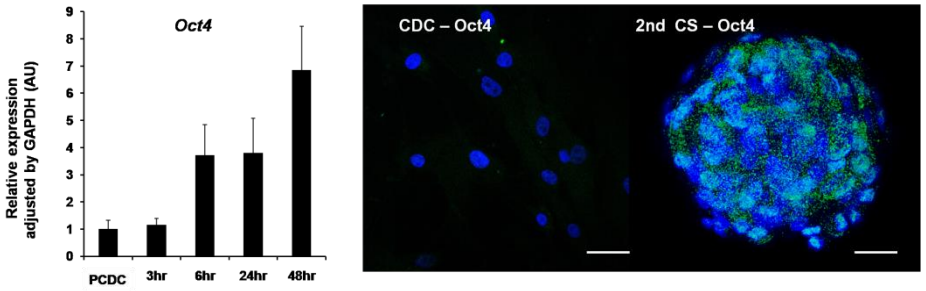

Figure 1-6 Difference in stemness between human CDC and secondary cardiosphere

(A) Secondary CSs were positive for alkaline phosphatase (ALP) staining, but the CDCs were not.

(B) Oct4 gene expression in CDCs and secondary CSs. Formation of secondary CSs up regulated the expression of Oct4 gene and protein. Bar: 50 mm.

A

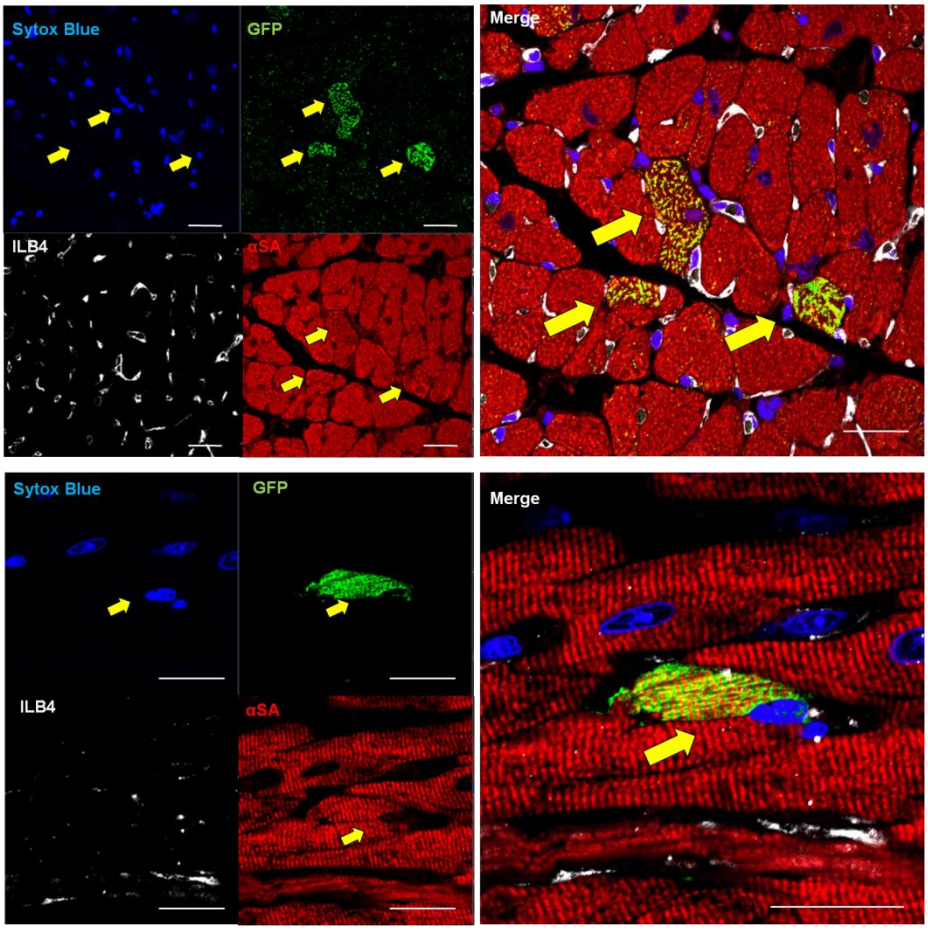
Sytox Blue
GFP
Merge
ILB4
αSA
Sytox Blue
GFP
Merge
ILB4
αSA

B

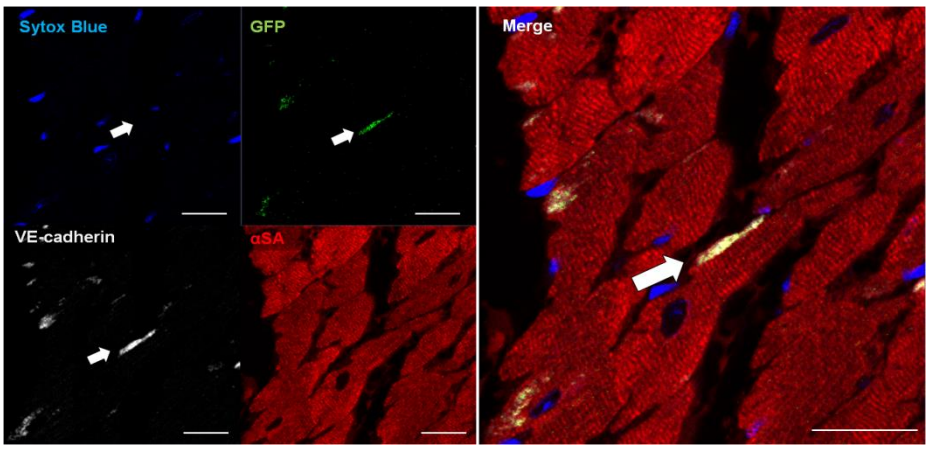
Sytox Blue
GFP
Merge
VE-cadherin
αSA

Figure 1-7 Transplantation of human secondary CSs into the ischemic heart

(A) GFP (+) secondary CSs differentiated into cardiomyocytes at post-transplantation day 14 (yellow arrows). (a-SA, alpha sarcomeric actinin; ILB4, isolectin B4) Bar: 20 mm.

(B) Some GFP (+) secondary CSs expressed VE-cadherin (+) at the peri-infarct sites, indicating endothelial differentiation (white arrow). Scale bar: 20 mm.

Table

Table 1-1 Comparison of four techniques to generate secondary cardiospheres

Secondary CS's	Poly-D-Lysine	Hanging-drop	Petri dish	AggreWell™
size (diameter)	50 - 200 μm (variable)	100 μm < (homogeneous)	50 - 200 μm (variable)	100 μm < (homogeneous)
mature time	72 hrs	12 ~ 48 hrs	72 hrs	3 ~ 24 hrs
handling time	very fast	long	very fast	fast
labor	simple	time consuming	simple	easy & simple
cost	expensive	inexpensive	inexpensive	expensive
product yield per dish	low	low	medium	high
sphere number (per 1 x 10^5)	50 - 100	50	100 - 200	1,000

DISCUSSION

As the search for optimal cell types continues, it has become increasingly clear that efforts to optimize the processing of cells for transplantation have been lagged. Because the very limited number of resident adult cardiac progenitor cells are acquired from biopsy tissues (5, 6), *in vitro* and *ex vivo* expansion of these cells is necessary for further application. To address this limitation, I have undertaken development of an optimal processing strategy for *ex vivo*–expanded cardiac progenitor cell. I have subsequently shown that murine and human secondary cardiospheres (CSs) generated from cardiosphere–derived cell (CDC), through repeated three–dimensional (3D) sphere formation, constitutes a simple but effective strategy capable of improving therapeutic efficacy.

Primary sphere formation and subsequent secondary sphere generation are a privilege of neural stem cells (21–23). Stem/progenitor cells in secondary neurosphere retain proliferation and differentiation potentials whereas cells in the attached condition readily lose these potentials (21). Consistent with neurosphere study, this result shows the primary CSs express the multipotency markers, but that CDCs gradually lose

these expressions, suggesting that cellular potency is likely to diminish when sufficient cell numbers are acquired using conventional 2-dimensional expansion. Thus, I generated secondary CSs from CDCs using 3-dimensional culture. Secondary CSs have restored Oct4 and c-kit expressions and exhibited potent differentiation potentials, indicating that repeated sphere formation may be useful for selecting stem/progenitor cells, eliminates differentiated cells, and provides a microenvironment mimicking *in vivo* niche(24).

So, I here demonstrated that; 1) primary CS express Oct4 and c-kit, but when expanded in a 2-dimensional culture system, CDC lose these characteristics, 2) using the 3-dimensional sphere formation strategy, secondary CS can be generated from monolayer CDCs, re-gain the expressions of multipotency markers and effectively differentiate into cardiovascular lineages, 3) secondary CS transplantation promotes cardiac repair after MI more efficiently than CDC transplantation by increasing cellular engraftment, cardiovascular differentiation, endogenous cardiac stem/progenitor cell activation, and neovascularization by humoral factor secretion.

To summarize, I described a simple but effective means of facilitating cardiac stem/progenitor cell-based therapy. The generation of human secondary CS from such as endomyocardial biopsy specimen of the patient was also evaluated for stemness potency. I here reported the possibility of therapeutic benefits of secondary CS. These findings suggest that secondary CSs possess greater differentiation potential to endothelial cell and cardiomyocyte than CDC.

CHAPTER 2

Application of molecular mechanism under the niche of sphere generation

INTRODUCTION

It was my aim to undertake the optimizing process strategy for *ex vivo*-expanded cardiac progenitor cells through repeated three-dimensional sphere formation (murine and human secondary cardiosphere). When the cardiosphere was generated, stemness related gene expression was increased. Moreover, cardiosphere could promote the neovascularization potential (6). It was necessary to investigate on the mechanism of sphere generation which promoted neovascularization, to use it as a potential source for cell-based therapy. I suggested that enhancing the stemness potential and promoting the secretory activity for paracrine effects are mutually exclusive routes. To prove this, there were two hypotheses: 1) it is important to enhance the cardiopoietic regenerative potential to promote infarct repair and, 2) promoting the secretory paracrine humoral effect to protect infarcted myocardium are separate routes. I investigated the therapeutic effects of two divergent cell-processing methods to enhance cellular potency and paracrine activities according to these hypotheses.

MATERIALS AND METHODS

1. Analysis of gene and protein and signaling pathways during generation of secondary cardiosphere

Microarray: Global gene expression analyses were performed using Mouse Whole-genome BeadChips® (Illumina). Samples were prepared as described by the manufacturer. To detect different probes (differentially expressed genes; DEG) among XX, YY, and ZZ, one-way ANOVA was used and Benjamin & Hochberg False Discovery Rate (FDR) was used. Significance was accepted for FDRs of < 5% and p-value of < 0.01. Cells were harvested and total RNA was extracted using TRIZOL (Life Technologies).

RT-PCR: Conventional RT-PCR and quantitative real-time PCR were performed using ABI7200® (Applied Biosystems). Total RNA was extracted using TRIZOL (Life Technologies).

Western blot: Protein extracts (20 μg per sample) from cells were separated by SDS-PAGE (Bio-Rad Laboratories) and electro-transferred. Membranes were probed with E-selectin (Santa Cruz), total/phosphor-AKT (Cell Signaling), total/phosphor-ERK (Cell Signaling), Sp1 (Santa Cruz), and

α-tubulin (Calbiochem) antibodies.

ELISA: To check VEGF secretion, cells were cultured in cytokine-free, 0.5% FBS containing media (35% IMDM and 65% DMEM/F12) 24 hours before experiments. Supernatants were collected and ELISA was performed according to the manufacturer's instructions (R&D Systems).

For signal blocking experiments, I applied U0126 (40 μM A.G.Scientific) to block ERK (25), LY294002 (10μM A.G. Scientific) to block AKT(26).

2. Optimize the two types of culture condition applied signaling pathways

To optimize the culture condition to escalation of stemness or paracrine effect, I applied the receptor tyrosine kinase-1 inhibitor PD153035 (20 μM, A.G. Scientific) and transforming growth factor-β receptor antagonist SB431542 (10 μM, TOCRIS bioscience). For stimulation of the ERK pathway EGF (25 ng/ml), TGF-β (10 ng/ml), VEGF (5 ng/ml) and basic fibroblast growth factor (bFGF, 40 ng/ml) were added to the culture medium.

3. Cell tracing of two differently-processed human secondary CSs in ischemic myocardium

Fluorescence nanoparticles (NEO-STEM™, Biterials) were used to trace the transplanted cells *in vivo*. The CGM containing nanoparticles were added to the CDC being cultured with CGM by 1:10 dilution. The next day, the CGM medium was changed and secondary CSs were generated with a mixture of cytokines and intracellular signaling inhibitors. The RITC labeled particles (red color) were applied for the stemness escalation condition while the FITC labeled particles (green color) for the paracrine enhancing condition.

4. Statistical analysis

All data are presented as the mean ± S.E.M. Statistical analyses were performed using the Student's t-test or one-way analysis of variance with Bonferroni's correction for intergroup comparisons. SPSS version 19.0 (SPSS, Chicago, IL) was used and P values <0.05 were considered to denote statistical significance.

RESULTS

Induction of E-selectin expression is indispensable to initiation of sphere formation

I investigated the molecular mechanisms responsible for sphere formation. By microarray, I examined and normalized 25,697 probes. By 1-way ANOVA, I chose 5,948 genes which were differently expressed among 3 time points. Thereafter, I selected early-responsive 591 genes which were up regulated in 6 hr compared with 0 and 48 hr. Among 591 genes at the initiation phase of sphere formation, I focused on cell-cell adhesion pathway because dynamic interactions through cell-cell contacts have been known to be important for stem cell maintenance (27). Using Gene Ontology database (www.geneontology.org), I selected 12 candidate genes (Figure 2-1A), and I finally focused on E-selectin because the gene expression of E-selectin was found to be up regulated in primary CSs, whereas its expression was minimal in CDCs. During the generation of secondary CSs, E-selectin was induced as early as 3 hours after sphere initiation (Figure 2-1B, Upper panel). I confirmed the protein expression of E-selectin by immune fluorescence 3-D confocal imaging (Figure 2-1B,

Lower panel). To address causal relationships and functional significance of E-selectin, I harvested hearts from E-selectin knock-out (KO) mice which were viable and fertile but impaired angiogenesis and post-natal vasculogenesis (11). The sphere was not generated (Figure 2-1C). Taken together, these data indicate that the induction of E-selectin expression is indispensable to sphere initiation.

E-selectin/ERK/VEGF auto-paracrine signaling loop is responsible for sphere formation

I next analyzed the key signaling pathway responsible for sphere formation. Neurosphere studies have suggested that PI3K/AKT and MAPK/ERK signaling pathways are required for sphere maintenance and stem cell survival (28, 29). When secondary cardiosphere was initiated, I found that the ERK pathway was activated whereas the AKT pathway was slightly suppressed (Figure 2-2A, Left panel). Next, when the ERK pathway was blocked (U0126), E-selectin expression decreased and sphere formation was retarded, but AKT inhibition (LY294002) did not affect sphere formation (Figure 2-2A, Right panel). In addition to measuring the average

sphere area following each pathway blocking, I also counted the number of cells per sphere. I hung drop 5,000 cells, and 48 hours later, I dissociated each sphere and counted cell numbers. Control group showed 5,572 ± 655 cells/sphere, whereas ERK-blocked group showed 525 ± 156 cells/sphere ($P<0.01$). However, AKT-blocked group revealed no significant decrease of cell numbers, compared with control group (4748 ± 582 cells/sphere, $P>0.05$). Taken together, these data indicated that the ERK/E-selectin pathway is, at least in part, responsible for sphere initiation. Sp1 was subsequently down-regulated after blocking ERK pathway (Figure 2-2A, Left panel). Sp1 is a well-known transcription factor of VEGF (30, 31). Thus, I checked VEGF expression. The mRNA expression of VEGF was markedly up regulated from 6 hours after sphere formation, and these expression levels were subsequently maintained (Figure 2-2B, Left panel). A secreted form of VEGF protein was up regulated 20-fold at 24 hours after sphere formation and further augmented at 72 hours in conditioned media from secondary CSs, indicating that secondary CSs secrete substantial amounts of angiogenic factors as compared with CDCs (Figure 2-2B, Right panel). Moreover I found ERK

inhibition markedly down regulated VEGF expression 24 hours after sphere initiation (Figure 2-2C, Left panel). Furthermore, when VEGF was blocked by siRNA, sphere maturation was remarkably decreased (Figure 2-2C, Right panel). These findings indicate that an ERK-dependent Sp1 pathway plays a key role in VEGF synthesis and that VEGF auto-paracrine loop is responsible for sphere maturation.

Similar propensity of mechanism of human secondary cardiosphere formation

To examine signaling pathways potentially involved in human secondary CS formation, I applied same blockers used mice studies; U0126 to block MAPK/ERK pathway(25) and LY294002 to block PI3K/AKT pathway(26). The AKT-blocked cells showed no significant differences in the size of the spheres produced compared to the controls, but the ERK-blocked cells showed a significant retardation in sphere formation. CDC incubated with an anti-VEGF blocking antibody showed a significant decrease in sphere formation (Figure 2-3A). These findings demonstrate that activation of the ERK and VEGF pathways are also required for the generation of human

secondary CSs.

Roles of cytokines and ERK pathway during human secondary cardiosphere generation

In comparison with monolayer-cultured CDCs, both *Oct4* and *Nanog* (representative stem cell markers) gene were markedly up regulated in secondary CSs (Figure 1-6B). Cardiosphere growth medium contains EGF, bFGF and when I generated secondary CSs under the cytokine-deprived conditions, I found that secondary CSs displayed greater stemness-related gene expression (Figure 2-4A). These data suggest that cellular differentiation and proliferation might be influenced by EGF and bFGF which bind to receptor tyrosine kinase.

Consequently, I speculated that a downstream signaling pathway may activate or inhibit cellular potentials during secondary sphere formation. Upon inhibition of the extracellular-signal-regulated kinase pathway during 3D sphere formation, *Oct4* expression increased and *VEGF* expression was markedly decreased, indicating that the ERK pathway is directional with respect to cellular potency or paracrine capacity (Figure 2-4B). These findings imply that

enhancing the cardiopoietic regenerative potential of cultured cells and promoting the secretory activity of cells for paracrine humoral effects are mutually exclusive routes, given a single *in vitro* processing condition.

Two differently-processed human secondary CSs

Divergent cell processing strategies were pursued with the idea that their combined use to enhance cellular potency and humoral activity, respectively, would be desirable to maximize therapeutic benefits of transplanted cells. The study hypothesis is illustrated in Figure 2-5A. The direct inhibition of ERK by U0126 resulted in hindrance of cells formation of 3D spheres. Therefore, various combinations of indirect ERK inhibitory or activating conditions were evaluated that did not altering 3D sphere formation. Condition A (Figure 2-5B) represents two-dimensional (2D) culture of CDCs on a fibronectin-coated dish. To create a 3D environment, I utilized a 48-hour hanging drop technique or the 24-hour AggreWell™ method. Our hypothesis of the optimal condition for transplantation was tested by generating six types of secondary CSs from CDCs.

I first compared the respective gene expression levels.

Inhibition of the ERK pathway during secondary CS generation by selectively blocking receptor tyrosine kinase-1 (RTK-1) and transforming growth factor-β (TGF-β), plus withholding epidermal growth factor (EGF) from culture medium (Figure 2-5B, cell processing condition D), resulted in a 20-fold increase in *Oct4* gene expression compared to the 2D monolayer-cultured CDCs (condition A, Left panel). Conversely, when the ERK pathway was stimulated by addition of EGF, TGF-β, VEGF, and basic fibroblast growth factor (bFGF) to the culture medium, *VEGF* expression was up regulated (Figure 2-5B, Right panel condition G). The levels of Oct4 and VEGF protein expression were also assessed by confocal imaging (Figure 2-5C) and there was significantly increased gene expression of *Oct4* in condition D and of *VEGF* in condition G, compared with secondary CSs in condition B. Therefore, condition D would likely be optimal for cardiopoietic regenerative purposes and condition G would likely be optimal for paracrine secretory activation.

Combined transplantation of two differently-processed human secondary CSs into ischemic myocardium

The effects of the two distinctly different processing techniques were examined on *in vivo* cardiac function after transplantation of the secondary CSs into the infarcted myocardium. The dual-purpose secondary CSs (conditions D and G) were then jointly transplanted into the peri-infarct areas (total 2,400 spheres, 1,200 spheres per condition from 1.5 x 10^5 CDCs). To further compare processing variations, identical cell numbers and volumes of conditions A (CDCs) and B (general secondary CSs) were injected, as well as PBS.

Left ventricular (28) size and function was assessed at day 14 after MI induction and cell transplantation. The echocardiographic exam showed significantly smaller LV dimensions at both systole and diastole and LV systolic function fared comparatively better with combined transplantation in terms of fractional shortening and ejection fraction (Figure 2-6A, Upper panel), suggesting the preservation of myocardium and the prevention of detrimental remodeling and after MI. The hearts were subsequently harvested for histologic preparations. To reflect physiologic dynamics, Masson's trichrome stain revealed that LV dimension and thickness were better preserved and the area of fibrotic infarct was significantly less

with combined transplantation (Figure 2-6A, Lower panel). These data indicate that combined processing of secondary CSs (conditions D and G) achieves maximal therapeutic benefits.

The neovasculogenic effect of combined transplantation of secondary CSs

For *in vivo* tracing, cells processed under conditions D and G were differentially tagged by green and red fluorescence nanoparticles (Figure 2-7A). The *in vivo* implications of secretory humoral effects were evaluated. In the peri-infarct area at day 14, the degree of neovascularization was measured by counting capillary vessels using endothelial cell-specific isolectin B4 (ILB4) stain (Figure 2-7B). Transplantation of CDCs (condition A) or secondary CSs that were generated under condition B showed significant angiogenic effects, compared to injection of PBS. However, combined transplantation of secondary CSs (conditions D and G) showed an additional increase in capillary density.

The cardiopoietic regenerative effect of secondary CSs

I also examined the *in vivo* cardiopoietic regenerative effect of

cells by potency escalation under condition D processing. To detect the differentiation capability of these progenitors to cardiomyocytes with fine striated sarcomere structure at day 14, secondary CSs under condition D (escalation of stemness potential) were tagged by a green fluorescence protein (GFP)-expressing lentivirus and co-transplanted with the unlabeled secondary CSs under condition G (enhancement of paracrine activity). Cells of secondary CSs processed under condition D differentiated to α-sarcomeric actinin (+) cardiomyocyte-like cells in the peri-infarct zone (Figure 2-8A).

A

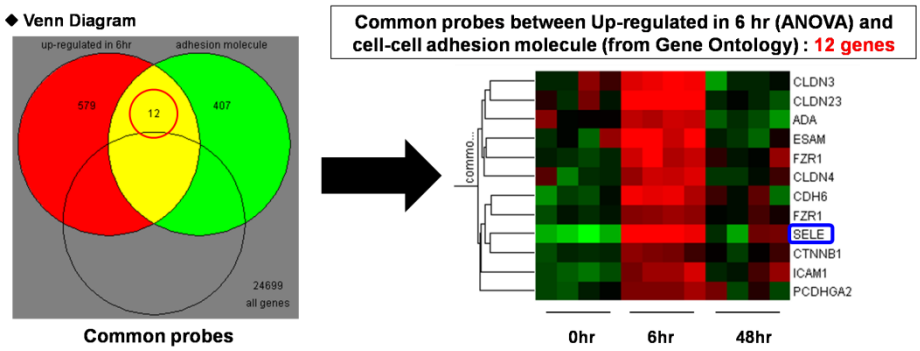
◆ Venn Diagram
up-regulated in 6hr
adhesion molecule
579
12
407
24699
all genes
Common probes
Common probes between Up-regulated in 6 hr (ANOVA) and cell-cell adhesion molecule (from Gene Ontology) : 12 genes
commo...
CLDN3
CLDN23
ADA
ESAM
FZR1
CLDN4
CDH6
FZR1
SELE
CTNNB1
ICAM1
PCDHGA2
0hr
6hr
48hr

B

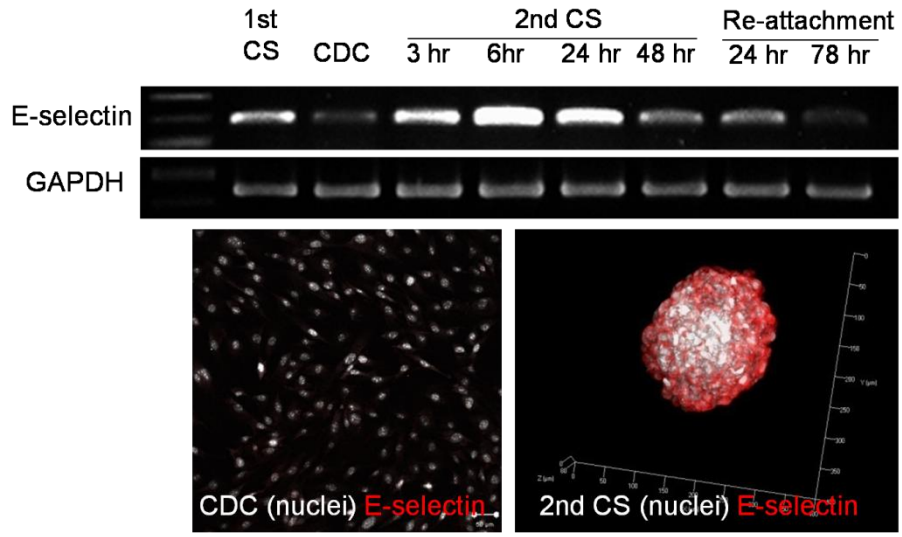
1st CS
CDC
2nd CS
3 hr
6hr
24 hr
48 hr
Re-attachment
24 hr
78 hr
E-selectin
GAPDH
CDC (nuclei) E-selectin
2nd CS (nuclei) E-selectin

C

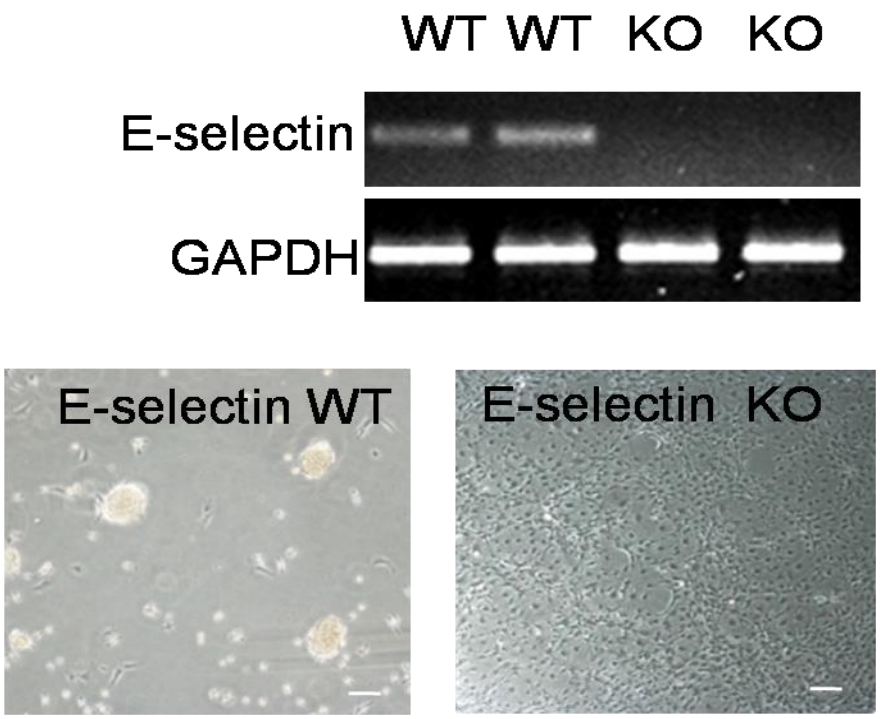

Figure 2-1 E-selectin expression in 2nd CS

(A) Using Gene Ontology database (www.geneontology.org), 12 candidate genes were selected which are known to be involved in cell-cell adhesion. SELE indicate E-selectin

(B) Primary CS and secondary CS highly expressed E-selectin, but CDC did not. Gene expressions were measured by RT-PCR and protein expressions were confirmed by immunofluorescence staining.

(C) The cells from E-selectin KO cardiac explant were not able to generate CSs. Bar: 200 μm.

A

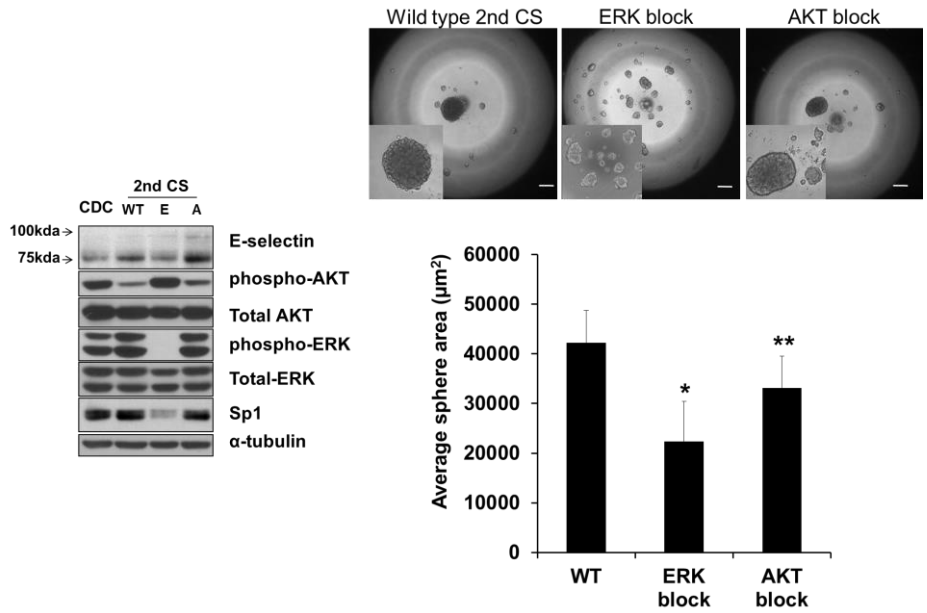
Wild type 2nd CS
ERK block
AKT block
2nd CS
CDC WT E A
100kda
75kda
E-selectin
phospho-AKT
Total AKT
phospho-ERK
Total-ERK
Sp1
α-tubulin
Average sphere area (μm²)
60000
50000
40000
30000
20000
10000
0
*
**
WT
ERK block
AKT block

B

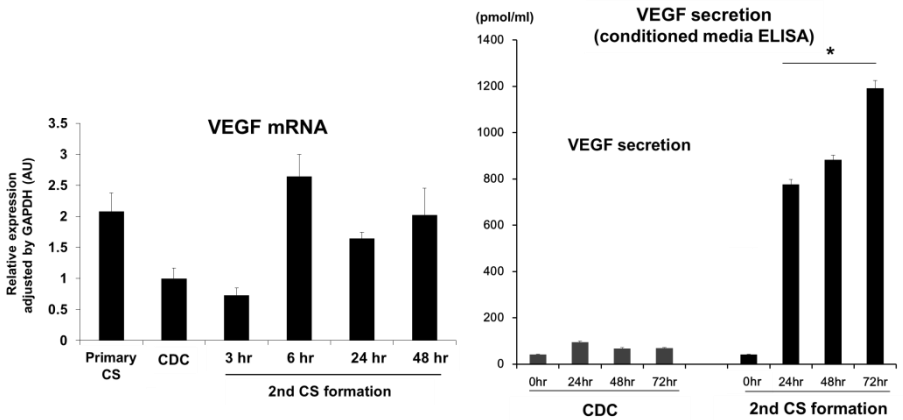
VEGF mRNA
Relative expression adjusted by GAPDH (AU)
3.5
3
2.5
2
1.5
1
0.5
0
Primary CS
CDC
3 hr
6 hr
24 hr
48 hr
2nd CS formation
(pmol/ml)
VEGF secretion (conditioned media ELISA)
VEGF secretion
1400
1200
1000
800
600
400
200
0
*
0hr
24hr
48hr
72hr
CDC
2nd CS formation

C

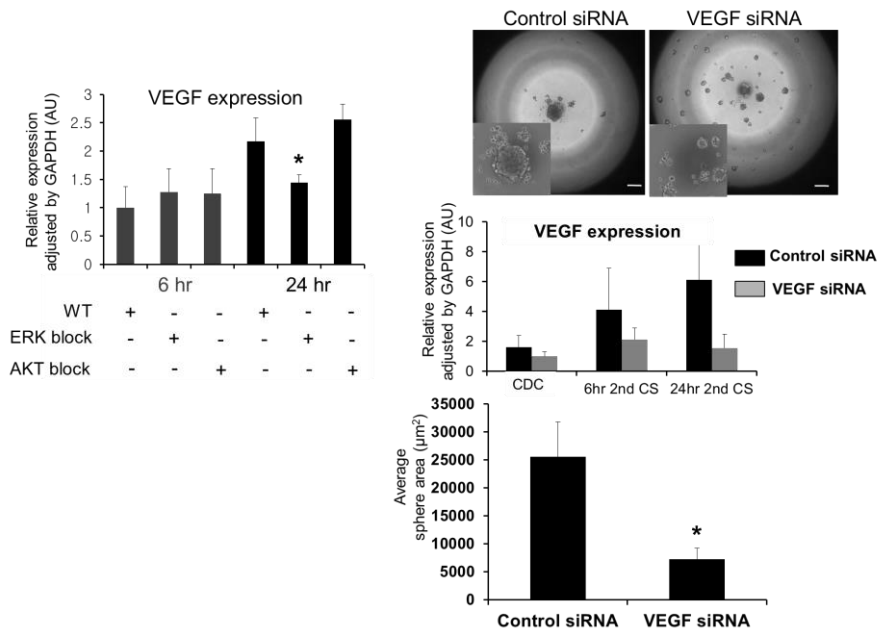

Figure 2-2 Molecular mechanisms of sphere formation

(A) Western blots at 12 hours after sphere formation demonstrated that E-selectin expression was induced following sphere formation. Blocking ERK pathway (E) suppressed E-selectin expression, but blocking AKT (A) pathway did not. When ERK was blocked, Sp1 was down regulated. Signal pathway blocking experiments demonstrated that the ERK pathway is responsible for sphere initiation and maturation. Average sphere areas were measured using pixel values (*P < 0.01, ERK block versus WT; **P > 0.05, AKT block versus WT). Bar: 200 μm.

(B) Real-time PCR of a representative cytokine, VEGF, of neovascularization. The secretion of VEGF protein into culture supernatant after sphere formation as determined by ELISA (n = 4; *P < 0.01, 0 hour versus 24 or 48 hours after sphere formation).

(C) After 24 hours, ERK inhibition significantly inhibited VEGF expression, indicating VEGF participates in the later stages of sphere formation (*P < 0.01, ERK block versus WT and versus an AKT block). Sphere maturation at 48 hours was markedly decreased by siRNA, targeting VEGF (*P < 0.01, control siRNA versus VEGF siRNA). Bar: 200 μm.

A

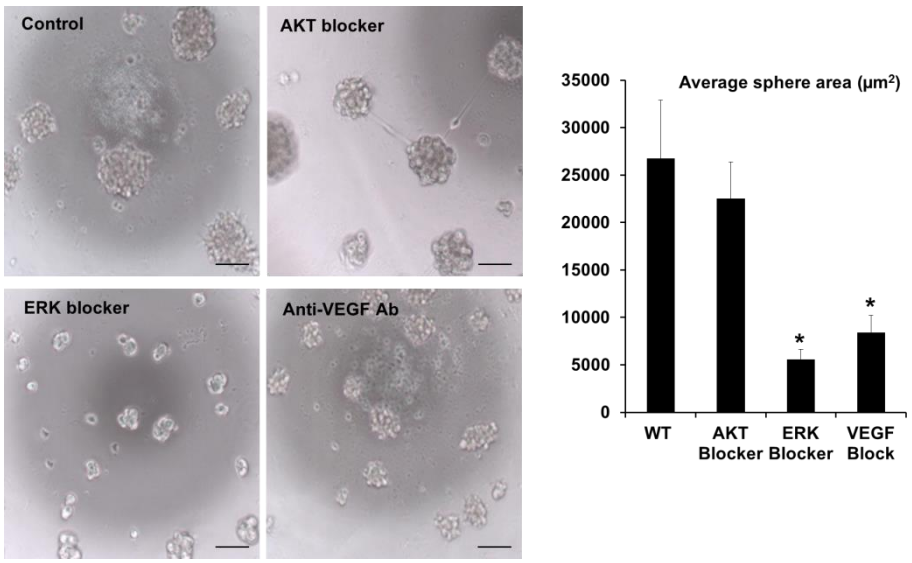

Figure 2-3 Mechanisms of human CSs formation: ERK and VEGF pathways

(A) Signal pathway blocking experiments demonstrated that the ERK pathway and VEGF are responsible for sphere formation (*P < 0.01 versus control).

A

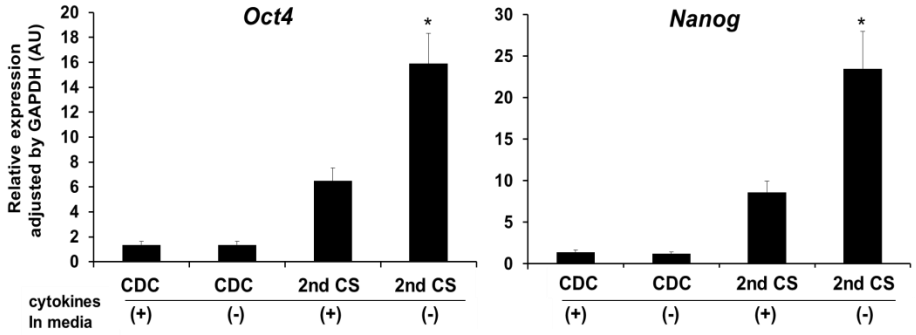

B

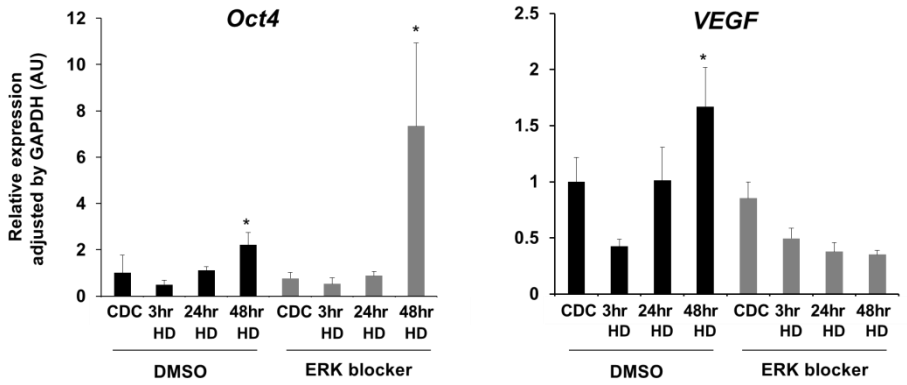

Figure 2-4 Expression of the stemness genes *Oct4* and *Nanog* under the cytokine-deprived conditions

(A) Addition of cytokine did not enhance the stemness gene expression. Intriguingly, in secondary CS generated by hanging-drop culture for 48 h, addition of cytokine mitigated the induction of *Oct4* and *Nanog* expression. Conversely, the stemness gene were enhanced under the cytokine-deprived conditions (*$P < 0.05$ versus secondary CSs with cytokines).

(B)Enhanced stemness and decreased secretory activity of secondary CSs under ERK inhibition. *Oct4* and *VEGF* expression, as determined by real-time PCR (*P < 0.05 versus CDC).

A

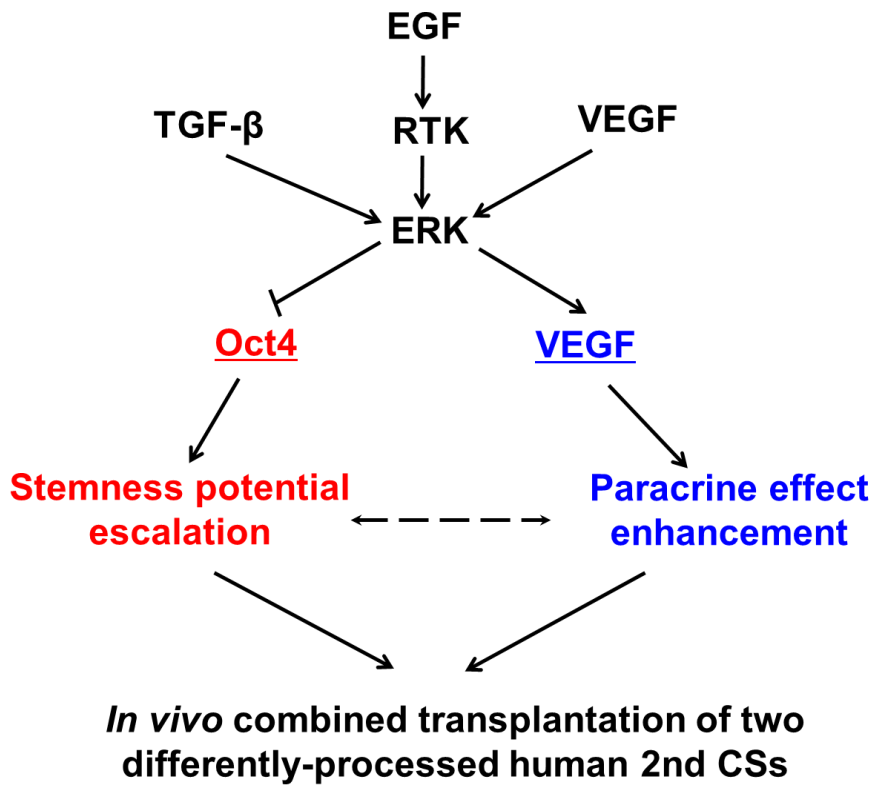

Figure 2-5 Two differently processed human secondary CSs

(A) The experimental scheme of different sphere generation

B

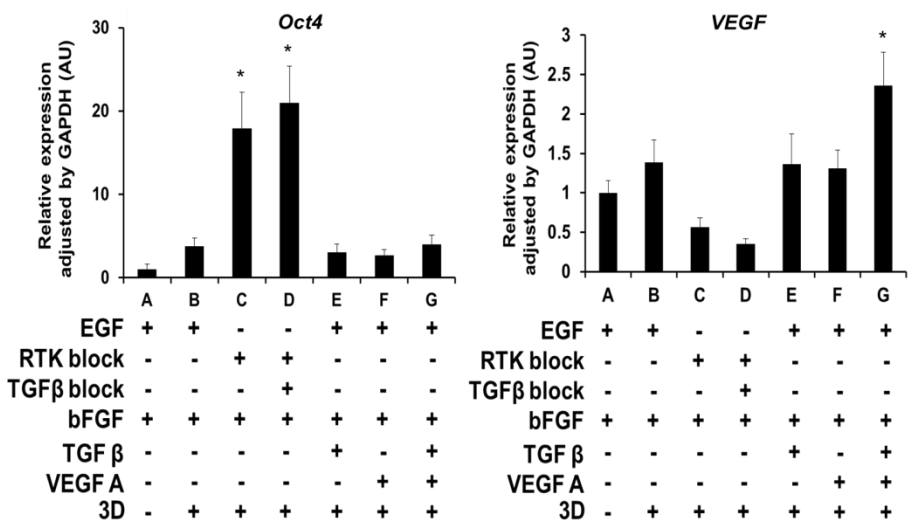

(B) Cell processing conditions A to G (Oct4 and VEGF expression as determined by real-time PCR). Condition A) primary cardiosphere-derived cells (CDC, 2D culture on fibronectin-coated dish); Condition B) generation of secondary cardiospheres from CDCs in 3D culture; Conditions C and D) stemness or regenerative potential escalation of secondary cardiospheres; and Conditions E – G) enhancement of paracrine effect Note: 3D culture was performed using the hanging drop method for 48 h.

C

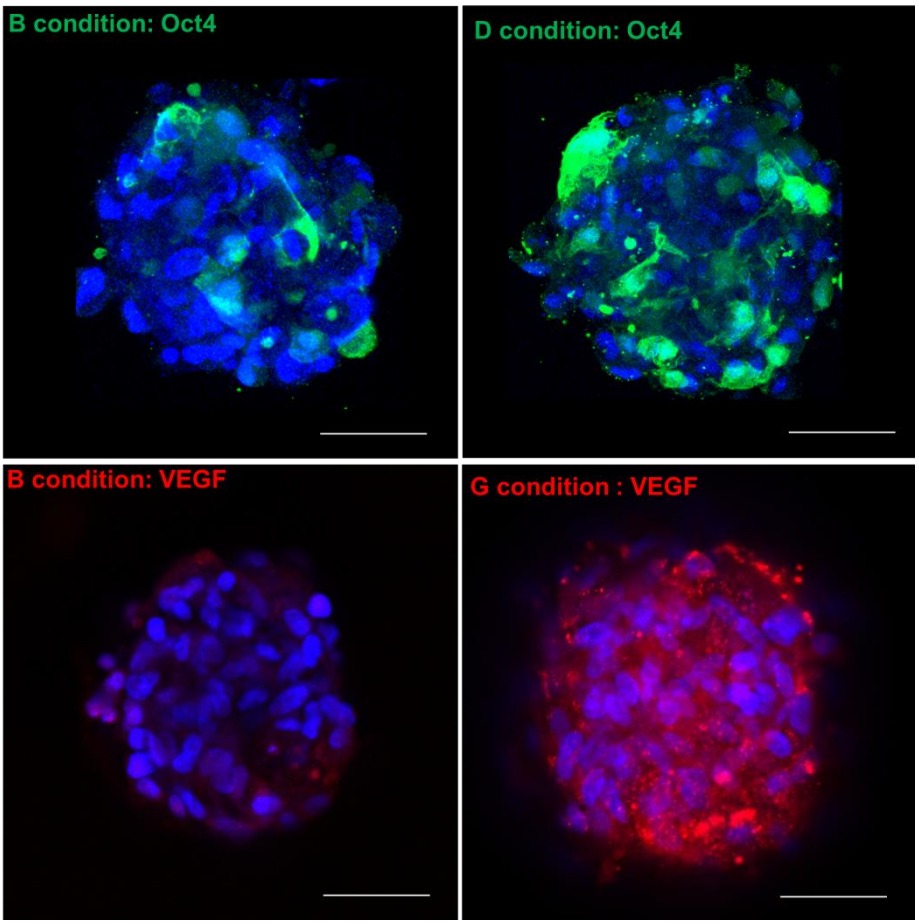

(C) Oct4 and VEGF protein expression visualized by confocal imaging. High Oct4 protein expression in secondary CSs under condition D processing (versus condition B); Increased VEGF expression under condition G (versus condition B). Bar: 50 μm.

A

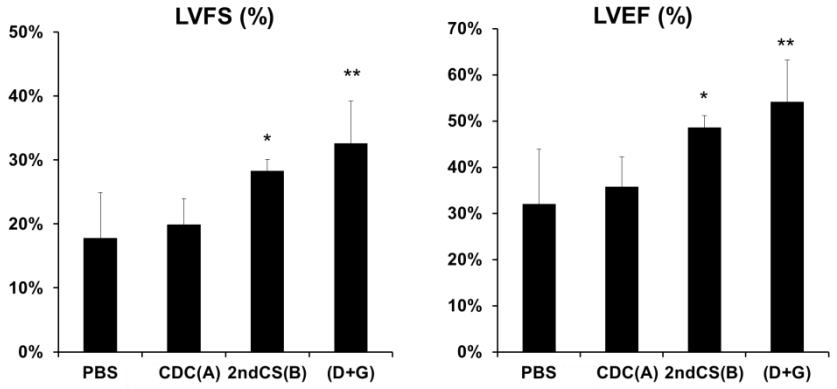
LVFS (%)
50%
40%
30%
20%
10%
0%
*
**
PBS
CDC(A)
2ndCS(B)
(D+G)

LVEF (%)
70%
60%
50%
40%
30%
20%
10%
0%
*
**
PBS
CDC(A)
2ndCS(B)
(D+G)

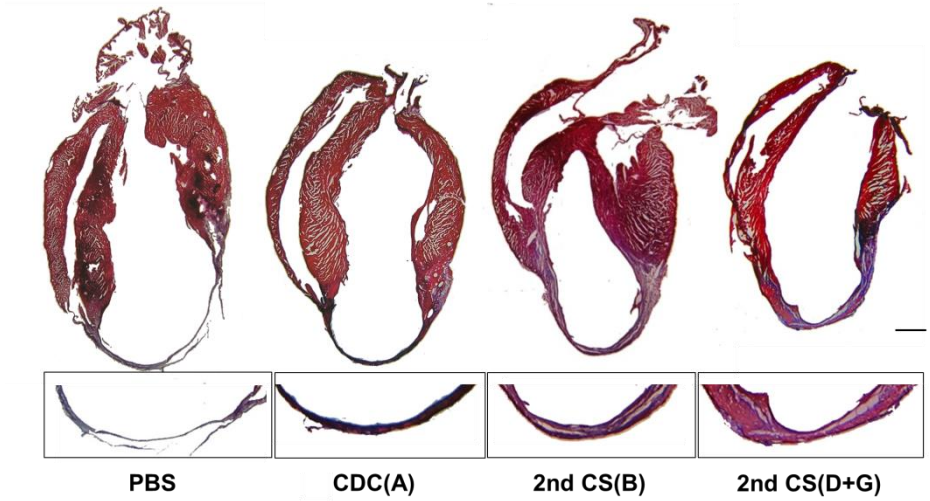
PBS
CDC(A)
2nd CS(B)
2nd CS(D+G)

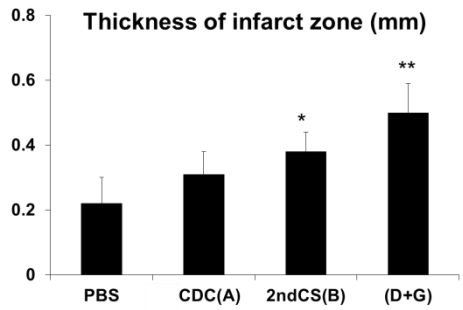
Thickness of infarct zone (mm)
0.8
0.6
0.4
0.2
0
*
**
PBS
CDC(A)
2ndCS(B)
(D+G)

Figure 2-6 Assessment of heart function after combined transplantation of secondary CSs

(A) Echocardiographic parameters at day 14. Combined transplantation of secondary CSs (D and G processing conditions) significantly improved left ventricular (28) function. LV fractional shortening (LVFS) and LV ejection fraction (LVEF) (*P < 0.05, **P < 0.01 versus PBS; Bar: 1000 μm). Combined transplantation of secondary CSs (D and G processing conditions) reduced infarct size and preserved LV of indication by Masson's trichrome staining.

A

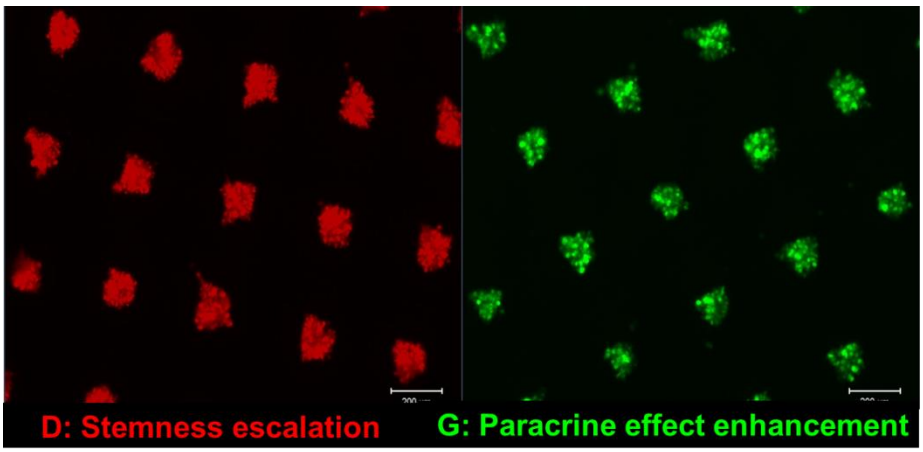

Figure 2-7 Neovasculogenic effect of combined transplantation of secondary CSs into infarcted myocardium

(A) Red- or green-colored nanoparticles denoting each of two different phenotypes of secondary CSs that were processed under condition D or G (one sphere = above 100 cells, Bar: 200 μm).

B

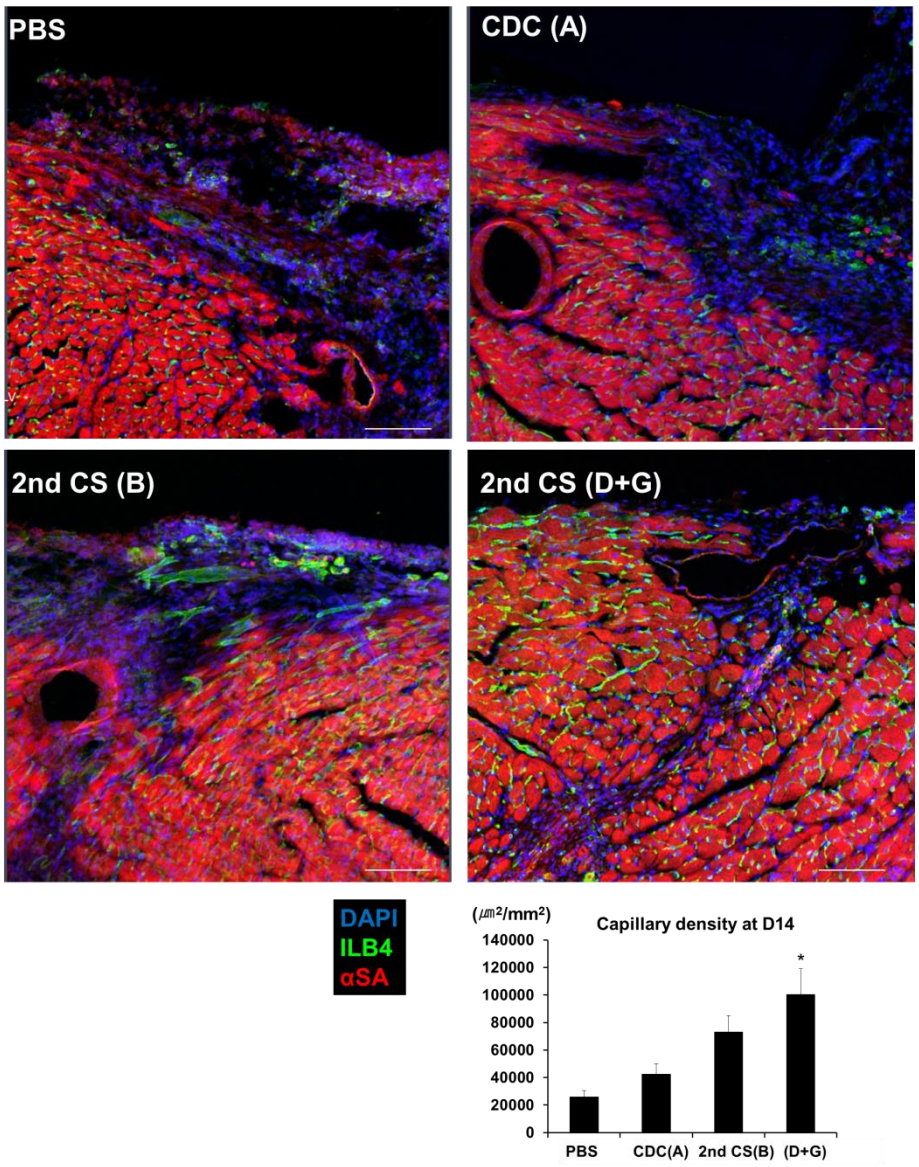

(B) Confocal microscopy assessment of capillary density at day 14 using fluorescent isolectin B4 (ILB4) stain (each n = 7, Bar: 50 μm).

A

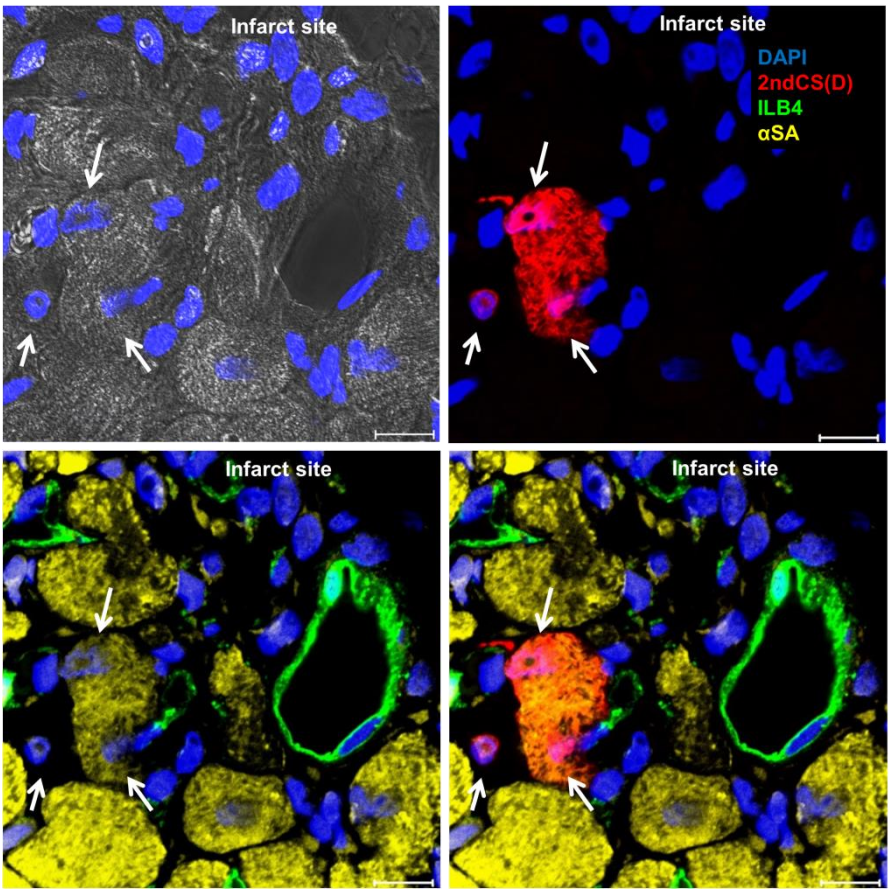

Figure 2-8 Differentiation of secondary CS into cardiomyocytes

(A) Secondary CSs processed under condition D (stemness escalation), tagged with GFP-expressing lentivirus and transplanted with the unlabeled secondary CSs processed under condition G (enhancement of paracrine activity). At day 14, a-sarcomeric actinin (+)/GFP (+) cells observed in peri infarct zone, suggesting the differentiation of progenitors to cardiomyocytes under condition D (Bar: 10 μm).

Tables

Table 2-1 Gene expression related to angiogenesis and vascular development (CDC versus 2nd CS)

Gene	0 hr	6hr	48 hr
VEGF-A	1	2.85	2.73
bFGF	1	2.53	2.46
Angiopoietin-2	1	3.01	1.39
Endothelin receptor type A	1	5.58	17.88
E-selectin	1	3.18	1.47
CXCL-1	1	1.86	1.36
IL-11	1	3.39	4.21
Growth differentiation factor 15 (GDF-15)	1	3.79	1.67
gremlin 1	1	3.07	5.86
Fms-like tyrosine kinase1 (Flt1)	1	1	0.97
B-cell translocation gene 1	1	2.46	3.66

DISCUSSION

The molecular mechanisms of sphere formation have remained elusive, although previous neurosphere studies have reported that PI3K/AKT and MAPK/ERK signaling pathways are involved in sphere maintenance and cell survival (28, 29). In this study, I hypothesized that sphere formation could be divided into two stages (sphere initiation and maturation). During an early stage, I presumed that adhesion molecules would play a critical role in cell-cell re-aggregation. Surprisingly, E-selectin expression was found to be induced as early as 3 hours after sphere formation. Furthermore, explant-migrating cells from E-selectin KO mice were not able to initiate cell-cell re-aggregation, and when E-selectin was knocked down by siRNA in wild type CDCs, sphere initiation was significantly retarded, indicating that the up regulation of E-selectin is indispensable to sphere initiation. Regarding the upstream signaling pathway involved, E-selectin expression was decreased and sphere initiation was retarded when ERK pathway was blocked. For sphere maturation, based on gene expression profiles at 48 hours after sphere formation, I hypothesized that auto-paracrine pathways were responsible. When the ERK pathway

was blocked, Sp1 was down regulated, and subsequently VEGF expression 24 hours after sphere initiation was markedly reduced. Furthermore, blocking VEGF with siRNA or antibody remarkably decreased sphere maturation, suggesting VEGF participates in the later stages of sphere formation. Together, I propose that ERK/E-selectin and ERK/Sp1/VEGF signaling cascades underlie sphere initiation and maturation. In this study, I found that 3D cardiosphere formation under cytokine-deprived conditions resulted in greater stemness-related gene expression but the sphere size was relatively smaller, implying that cellular differentiation and proliferation might be influenced by cytokines. In the niche, several growth factors and cytokines activate many signaling pathways through receptor tyrosine kinases and result in cellular proliferation or differentiation (32, 33). Among several pathways, previous reports have shown that ERK activation sufficiently induced neuronal differentiation as a core pathway (32). When I inhibited the ERK pathway completely using a specific blocker (U0126), Oct4 expression was significantly increased and VEGF expression was decreased. Interestingly, sphere formation itself was markedly retarded. Altogether, these data suggest that ERK inhibition

may boost “stemness” potential through inhibiting cellular differentiation and hinder sphere formation through inhibiting cellular proliferation, cell-to-cell adhesion and cytokine secretion. Therefore, I tested various combinations of ERK inhibitory or activating conditions and found two different optimal combinations of inhibitors and cytokines to enhance cellular potency (inhibition of ERK pathway by RTK-1, TGFβ inhibition) or augment secretory humoral activity (stimulation of ERK pathway by EGF, bFGF and VEGF). Furthermore, a recent study demonstrated that *in vitro* expansion of bone marrow-derived mesenchymal stem cells or c-kit (+) cardiac stem cells and subsequent *in vivo* combined transplantation enhanced infarct repair through synergistic biological interactions between two types of cells (34). In conclusion, combined transplantation of two different and purpose-oriented phenotypes of human secondary CSs under different (ERK inhibitory or activating) cell-processing conditions, enhances infarct repair through the complementary enhancement of cardiopoietic regenerative and paracrine humoral effects.

CHAPTER 3

LPAR4+ cardiac progenitor cells have therapeutic potency to repair ischemic heart disease

INTRODUCTION

An extensive investigation regarding cell-based therapy has been taken place in the purpose of improving functional cardiac repair (1, 35, 36). An optimal therapeutic cell type required for cardiac repair should satisfy the following conditions: 1) sufficient number, 2) high efficiency of cell engraftment when transplanted into injured heart, 3) possessing multi-potency to differentiate into cardio vascular lineage (4). It has become increasingly clear that efforts made to optimize the processing of cells for transplantation have not met an expected level (37, 38). The main reason is that because a very limited number of resident adult cardiac progenitor cells can be acquired from biopsy tissues, *in vitro* and *ex vivo* expansion of these cells is necessary for further application. However, it is hard to maintain pluripotent characteristic of the cells once out of living tissues (5, 6). To alleviate this limitation, I have found a secondary cardiosphere via 3-dimensional culture, which contributed much to the maintenance of pluripotency of adult cardiac progenitor cells *in vitro* and *ex vivo*. Nonetheless, the need for finalizing optimal cell conditions is continuously arisen to issue due to lack of reproducibility to reach a certain level of

differentiation potential. In contrast to embryonic stem cell or induced-pluripotent stem cells, adult cardiac stem cells are much difficult to maintain stemness property of which cellular potency to differentiate into cardiomyocyte is robustly retained. However, differentiation studies from mouse embryonic stem (mES) cells or induced pluripotent stem (iPS) cells into cardiomyocyte were better defined than using adult cardiac stem cells. Such conclusion led me to scrutinize further for other aspects of study results of embryo developmental stages with differentiation of iPS cells and I have found one target, Lysophosphatidic acid receptor 4 (LPAR4), which its function is not much unveiled during development.

The LPAR4 was first introduced in 2003 by Kyoko Noguchi *et al*. LPAR4 is one of G protein coupled receptor and distinct family from other LPA receptors. Amino acid identity of LPAR4 shares only 20-24% compared with LPA 1, 2, 3 families (9). LPAR4 was previously reported to be important for vessel formation during development stage and LPAR4-deficient mice showed dominant postnatal lethal phenotype and littermates were born with abnormal body tissue (39). Moreover, LPAR4 is also expressed in a rat embryonic heart during development

(40-42). Agonist of LPAR4 is Lysophosphatidic acid (LPA). Production of extra cellular LPA involves hydrolysis of lysophosphatidyl choline (LPC) by autotaxin (43), (44). Levels of autotaxin and LPA increase in mice after high-fat feeding (45). Moreover, there are several reports that autotaxin is observed in tumor tissue, and produced by adipose tissue. Autotaxin is in metastasis and invasion with cell migration (46). LPA is implicated in pathologic conditions such as atherosclerosis, hypertension and ischemic reperfusion injury. For example, cell migration and proliferation of fibroblast is stimulated through LPA/LPAR1 dependent manner. The LPAR1 has been introduced as a major pro-fibrotic mediator that is dependent on Rho down-stream signal in physiology and pathology (47-49). However, not just only LPAR4, LPAR1 was also essential for lymphatic vessel development (39, 50). In LPA/LPAR down-stream signal and its function, physiologic, pathologic function of LPAR4 still remains to be elucidated while LPAR1 has been widely studied (47-49, 51).

This chapter highlights the finding of LPAR4 expression in the mouse phase-bright cells which allowed us to investigate as one of cardiac stem/progenitor cells.

MATERIALS AND METHODS

1. Animals

Below 6 week C57BL/6J back grounded, β-actin promoter-driven eGFP expressing mice were used for isolation of phase-bright cells. Above 8 week C57BL/6J were used for myocardial infarction model. All animal experiments were performed after receiving approval from the Institutional Animal Care and Use Committee (IACUC) at Seoul National University Hospital, Seoul, Korea.

2. Staining whole body slice in early fetus

At embryo day 12.5, fetuses were extracted from a uterus. 6 to 9 fetuses were anesthetized with CO_2 gas. Embryo was soaked in 4% PFA for overnight at 4 ℃. Fixed tissue was embedded in paraffin. The paraffin block were cut into 4 ㎛ slice. Tissue section was incubated with LPAR4 (Santa Cruz Biotechnology, Bioss), α-Sarcomeric actinin (Sigma), DAPI (Invitrogen) antibodies. The positive signal was detected with confocal microscopy (Zeiss).

3. Detecting the adult cardiac stem cells from heart tissue

To find a cardiac stem cell from tissue, the mice heart was enzymatically dissociated to single cells by perfusion solution and perfusion system. The mice heart became to single cell via 3 steps. First, the heart blood was perfused through the aorta with Ca^{2+} free Tyrode buffer (NaCl 135mM, KCl 4mM, $MgCl_2$ 1mM, HEPES 10mM, NaH_2PO_4 0.33mM, PH=7.4 at RT) for 3 minutes (3CC/min). Next using perfusion buffer (added Glucose 10mM, butanedione monoxime (BDM) 10mM, Taurine 5mM, collagenase type Ⅱ 0.5mg/mice bodyweight (g) in Ca^{2+} free Tyrode buffer), heart was perfused for 10 minutes (3CC/min). Finally, heart was soaked in neutralization solution (added BSA 5mg/ml in perfusion buffer without collagenase type Ⅱ). Structural disrupted heart was torn in small pieces as possible with blunt forceps. The small pieces was flown through the strainers from 250 ㎛ to 40 ㎛ pore size gradiently. After washing, the cells were attached to slide glass using Cytospin (2000 rpm, 3 min). Cardiac stem cells were detected from confocal microscopy (Zeiss) after immune fluorescence staining (c-kit, LPAR4). To compare between these stained cells and phase-bright cells, the explant tissue was also stained.

4. Analysis of molecular expression pattern

FACS: For quantitative analysis of the LPAR4 + cells, FACS was performed. Single-dissociated cells from heart and phase-bright cells were incubated with LPAR4 (Bioss) and c-kit (e-bioscience). Analysis was performed using FACS Caliber (Becton Dickinson).

IF: Immunofluorescence staining was performed to find a location of expression. Analysis was performed using LSM 710, ZEN 2010 software (ZEISS).

PCR: To confirm the gene expression, RT-PCR and quantitative real-time PCR were performed using ABI7200® (Applied Biosystems). Total RNA was extracted using TRIZOL (Life Technologies).

Western blot: Protein extracts (20 μg per sample) from cells were separated by SDS-PAGE (Bio-Rad Laboratories) and electro-transferred. Membranes were probed with total/phosphor-ERK (Cell Signaling),

5. *LPAR4* gene knockdown and overexpression

Cardiosphere derived cells (1 x 10^5) were transduced with lentiviral particle coding for short hairpin (sh) RNAs against

LPAR4 gene. Puromycin of 20 μg/ ml was used for selection of surviving cells in 2 days after transduction. Doxycycline induced LPAR4 gene overexpression vector was packing into lentivirus to increase gene expression. The lentiviral vector was transduced into CDC.

6. Confocal Microscope

Immune staining image was acquired from LSM-710 confocal microscope (Zeiss) including X40 or X63 objective lens. The samples were exited with 405, 488, 543, 633nm laser light sources. To detect the true signal, the emission-signal was averaged after 4 times scanning by ZEN 2010 software (Zeiss).

7. Explant culture of 4 heart chambers, septum and apex

Mice heart was split into 6 sites of right atrium (RA), left atrium (LA), right ventricle (RV), left ventricle (LV), septum (SEP-between LV and RV) and heart apex (APX-end of heart) site (N = 10). Split sites of heart tissues were separately explant cultured. After about 2 weeks later, generated phase-bright cells were analyzed by FACS for LPAR4 expression.

8. Differentiation into cardiomyocyte

Right atrium of 5 to 6 week mice were dissected and cultured on the fibronectin-coated dish with complete explant medium (CEM). After 2 days, 1 μM LPA was treated to explanted tissue. About 2 weeks later, phase-bright cells were cultured on Aggrewell™ with 10ng/ml BMP4, 1 μM LPA. Next day, generated spheres were transferred to Ultra-low attachment dish with 10ng/ml BMP4, 10ng/ml Activin, 10ng/ml bFGF, 1 μM LPA for about 2 to 3 days for an exclusion of fibroblast cells. Floating sphere were attached on 0.1% gelatin-coated dish with cardiosphere growth medium (containing 5% FBS, 2% B27, 25 ng/ml EGF, 40 ng/ml bFGF, 4 ng/ml cardiotropin-1, 1 unit thrombin, 2 mM L-glutamine, 0.1 mM 2-mercaptoethanol) and 5 ng/ml VEGF.

9. Evaluation of differentiated phase-bright cells

After 7 days of culture under cardiomyocyte differentiation condition, Cell membrane was permeabilized by Flow Cytometry Fixation & Permeabilization Buffer Kit (R&D) and FACS analysis was performed by Caliber

(Becton Dickinson). Troponin-T, sarcomeric actinin (Abcam) and LPAR4 (Bioss) antibodies were used.

RESULTS

The LPAR4 expression in early embryo

LPAR4 was focused on microarray data previously acquired from our laboratory. To confirm the reference data, slice of whole fetus was stained with LPAR4 and α-Sarcomeric actinin (αSA). Almost none but only in heart area, strong positive signal was detected, especially LPAR4 and αSA, cardiac specific marker, were co-expressed in the heart (Figure 3-1A).

The LPAR4 expression in cardiac stem cells

I investigated on the cardiac stem cells in adult heart tissue using immunofluorescence staining. Some cells had an adult cardiac stem cell marker c-kit and Lysophosphatidic acid receptor 4 (LPAR4) merged signal, one of a G protein-coupled receptor, in enzymatic digested single cells from mice heart tissue (Figure 3-2A, Upper Left panel). However while a few cells were c-kit and LPAR4 double positive, some cells were LPAR4 and cardiomyocyte specific marker-α-sarcomeric actinin (αSA) double positive. But, the αSA was expressing on cell membrane site of weak LPAR4 expression (Figure 3-

2A, Upper Right panel). While some of cells express LPAR4 only, other cell were expressing stronger αSA (Lower Left). To compare the quantity of LPAR4+ cells in heart with phase-bright cells from explant culture, FACS analysis was performed. FACS result revealed there are about 5% LPAR4+ cells in whole dissociated cells from heart tissue (Figure 3-3A, Left panel). Due to its small number of total dissociated single cells that are LPAR4+ in heart tissue, I failed to isolate them. However, I checked the phase-bright cells, which was 40% of phase-bright cells from explant culture of tissue (Figure 3-3A, Right panel). Moreover, phase bright cells had more double positive in FACS analysis. It was discovered that almost all phase-bright cells expressed LPAR4 from immune staining results (Figure 3-3B). When LPA was treated(1μM, sigma) for a week to explanted tissue, more phase-bright cells were observed (Figure 3-4A, left panel). The secondary cardiosphere significantly had almost 10 times higher *LPAR4* gene expression than CDC had. *LPAR4* gene level of attached CDC was down regulated more compared to 3-dimensional cultured primary cardiospheres or secondary cardiospheres (Figure 3-5A).

Right atrium and Apex had superior Possibility to isolate the cardiac stem cells

Mice heart was split into 6 sites RA, LA, RV, LV, SEP and apex to evaluate the place for more phase-bright cell generation. In the majority of the right atrium and apex, there were more phase-bright cells than in any other sites. It was confirmed from FACS data that higher LPAR4 expression was observed when there were more phase-bright cells. In the atrium, phase-bright cells tended to be generated more than in the ventricle (N = 10). FACS analysis revealed that the phase-bright cells from RA and apex were expressed more than 90% LPAR4 (Figure 3-6A).

LPAR4+ phase-bright cells have more differentiation potency than CDCs have

Figure 3-7A is schematic figure for cardiomyocyte differentiation from LPAR4+ phase-bright cells. It is important to mass produce LPAR4+ phase-bright cells for differentiation and in order to do that, 1 μM LPA was treated to explant tissue per every media change when the generation of phase-bright cells began. When LPA was treated to explant tissue, more

phase-bright cells were generated and *LPAR4* gene expression was more than 3 fold higher than no LPA treated group (N = 3) (Figure 3-7B Upper Left). During the first aggregation step, LPAR4 was increased more as well as stem cell marker, *c-kit or Oct4* (Figure 3-7B Lower Left, Right). When the cells were attached to induce differentiation, LPAR4 was down regulated. But *troponin-t* gene began to be expressed even though it was weak, but it had higher expression of *troponin-t* gene than CDC had (Figure 3-7B Upper Right). To confirm this protein by immunofluorescence staining and FACS, troponin-t or α-sarcomeric actinin was detected. The result showed that the 15.2 % Troponin-T and 29.8 % Sarcomeric-alpha actinin+ with LPAR4 (Figure 3-7C, D n=3).

ERK activation was blocked by LPA/LPAR4

To investigate the relationship between LPAR4 and pERK, transduction of LPAR4 lentiviral vector was performed before LPA treatment. After 1 hour of LPA treatment, cell was harvested and proteins were extracted using RIPA buffer. Then, immunoblotting experiment was performed. LPAR4 overexpression blocked ERK phosphorylation. However, when

LPAR4 was down-regulated using shRNA lentivirus, ERK was activated (Figure 3-8A).

A

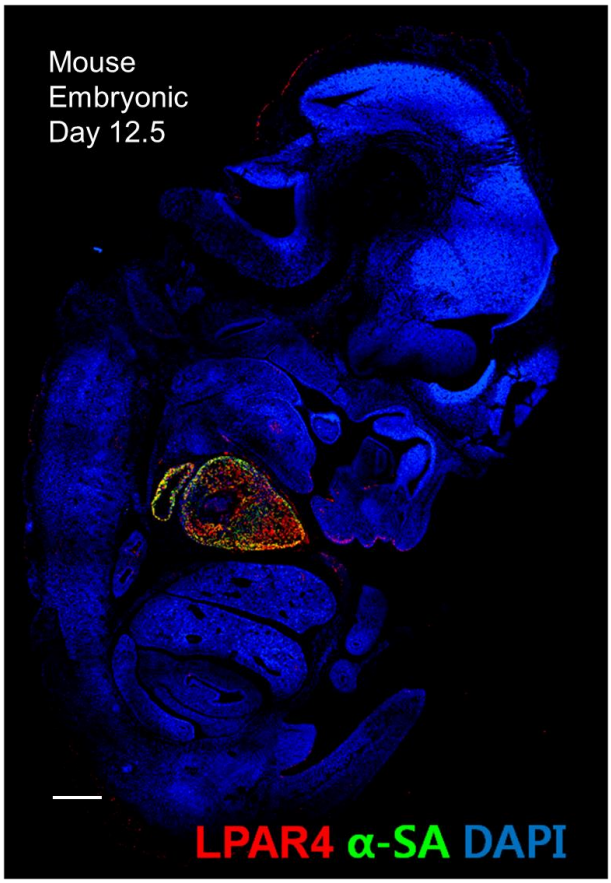

Figure 3-1 Paraffin slide of embryonic day 12.5 fetus with expression of LPAR4 in heart

(A) Paraffin block from embryonic day 12.5 fetuses were cut into 4 μm slices. Tissue section was incubated with LPAR4 (Santa Cruz Biotechnology), α-Sarcomeric actinin (Sigma Aldrich), DAPI (Invitrogen) antibodies. The positive signal was detected with confocal microscopy (Zeiss). LPAR4 is expressed in heart during developmental stage. Bar: 100 μm.

A

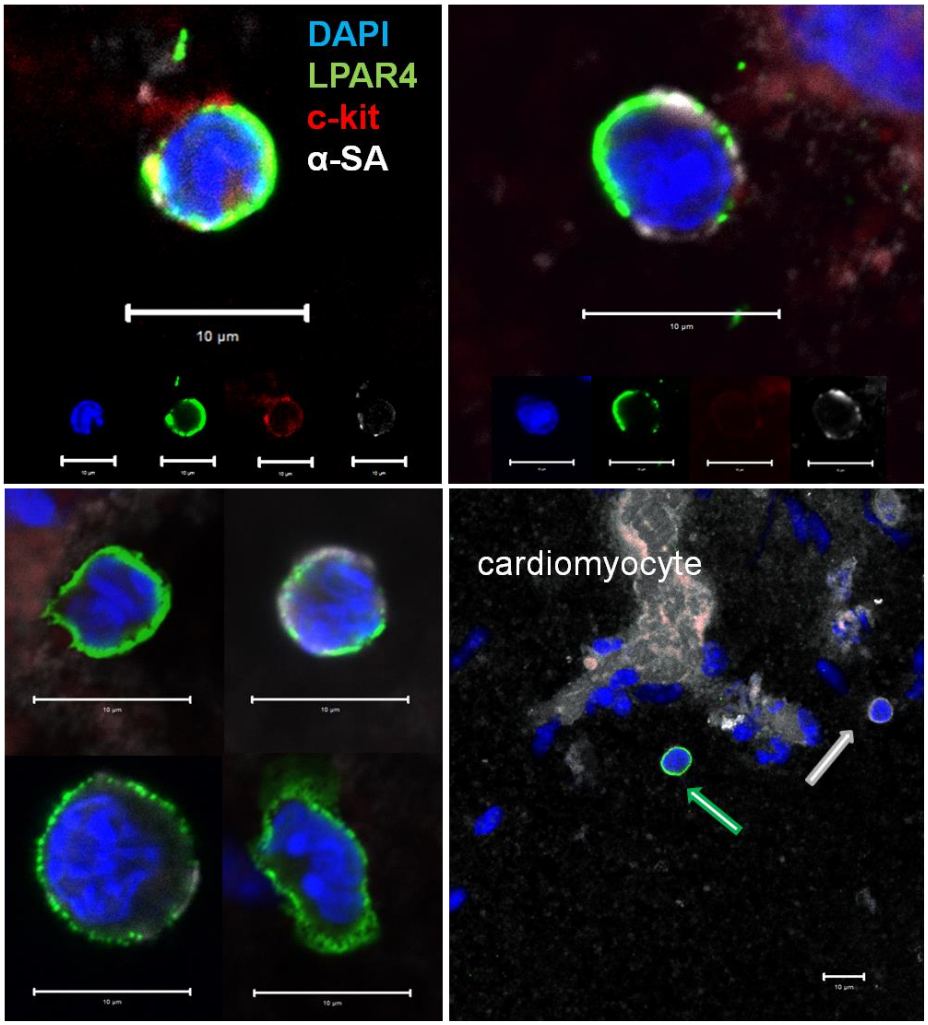

Figure 3-2 The LPAR4 expression in enzymatically dissociated single cells from heart

(A) Small number of cell were double-positive for adult cardiac stem cell marker c-kit and Lysophosphatidic acid receptor 4 (Upper Right). Some LPAR4+ cells showed co-

expression of cardiomyocyte specific marker－α－sarcomeric actinin (αSA). But, the αSA was starting to be expressed on cell membrane site with weak LPAR4 expression (Figure 3－2A, Upper Right panel). The sizes and diversity of cells were detected. While some cells expressed LPAR4 only, other cells were expressed stronger αSA (Lower Left). There was only LPAR4+ cell (green arrow) and only αSA+ (white arrow) cells in one field (Lower Right). Dissociated cell was attached to slide glass using Cytospin, cells were incubated with LPAR4 (Santa Cruz Biotechnology), α－Sarcomeric actinin (Sigma Aldrich), DAPI (Invitrogen) antibodies. The positive signal was detected with confocal microscope (Zeiss). Bar: 10μm.

A

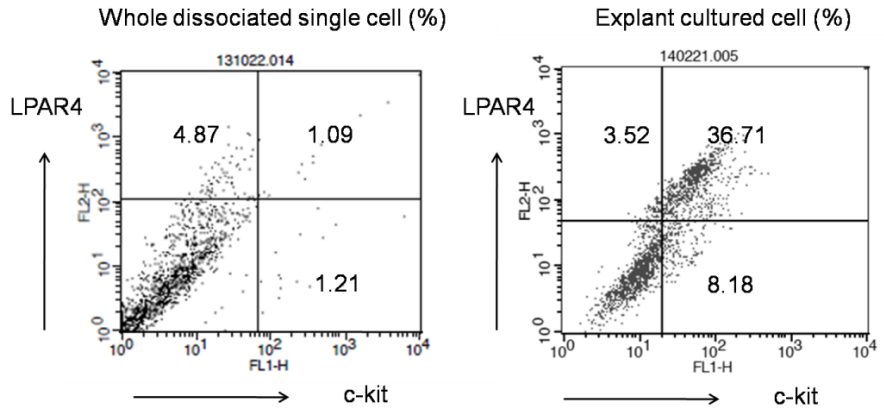
Whole dissociated single cell (%)
Explant cultured cell (%)
131022.014
140221.005
LPAR4
LPAR4
4.87
1.09
1.21
3.52
36.71
8.18
FL2-H
FL1-H
c-kit
c-kit

B

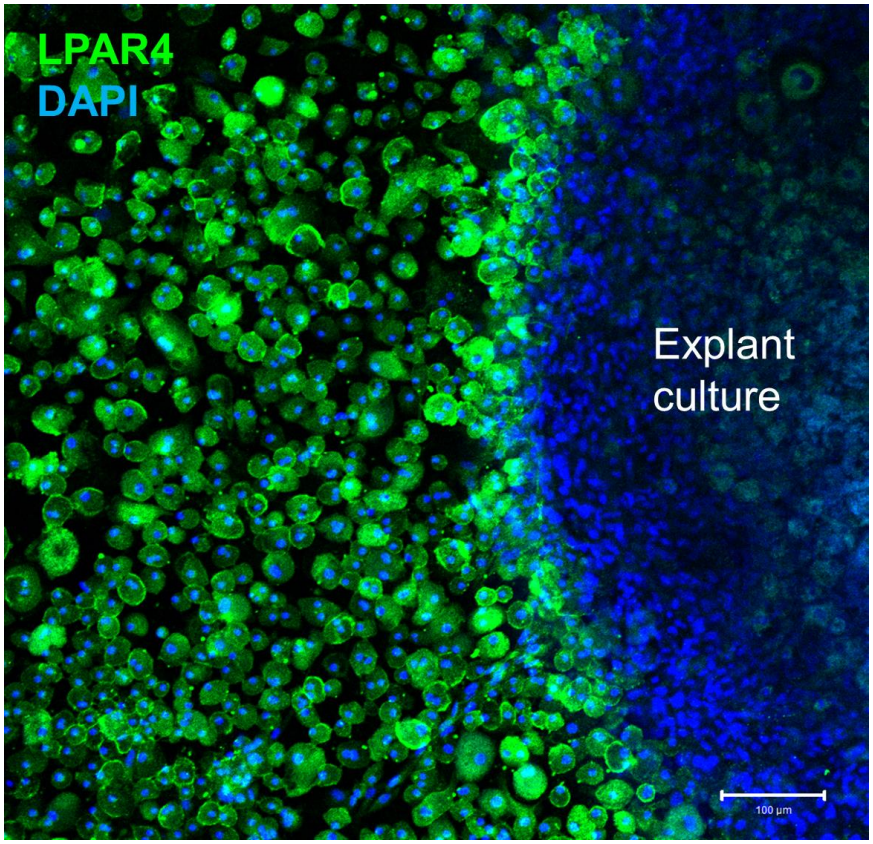
LPAR4
DAPI
Explant
culture
100 μm

Figure 3-3 Quantitation of LPAR4 in enzymatically dissociated single cells from heart and phase-bright cells and IF staining

(A) FACS analysis showed that dissociated single cells from heart and phase-bright cells expressed c-kit and LPAR4, but there was minor expression in dissociated single cells.

(B) Explant tissue was stained with LPAR4. The image shows LPAR4 is only stained in phase-bright cells while center of explant tissue are not. Bar: 100 μm.

A

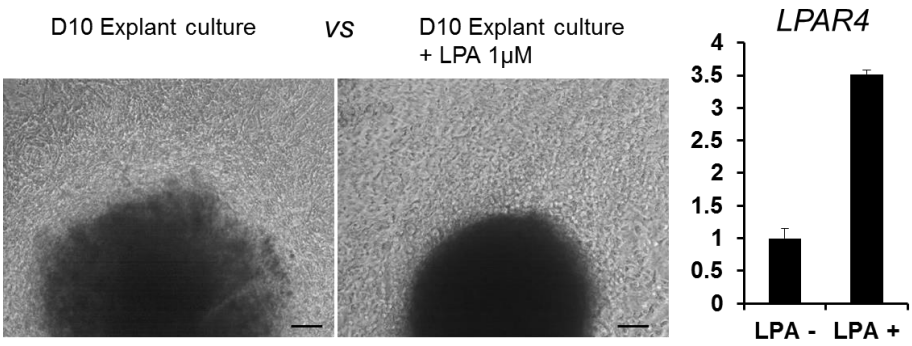

Figure 3-4 LPA have an influence on generation of phase-bright cells from explant tissue fragment

(A) More phase-bright cells were generated by 1 μM LPA and the *LPAR4* gene expression was more than 3 times higher. LPA was added every 2 days by changing of the LPA contained medium. Bar: 100 μm.

A

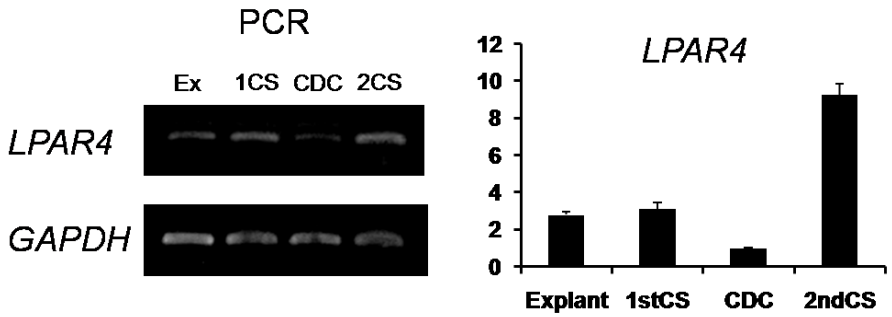

Figure 3-5 Conventional PCR and real time PCR result of LPAR4 gene from explant tissue to secondary cardiosphere

(A) *LPAR4* gene was increased about 10 folds in secondary CS than CDC. When cell was attached, *LPAR4* gene was more down regulated compared to 3-dimensional cultured primary cardiosphere or secondary cardiosphere.

A

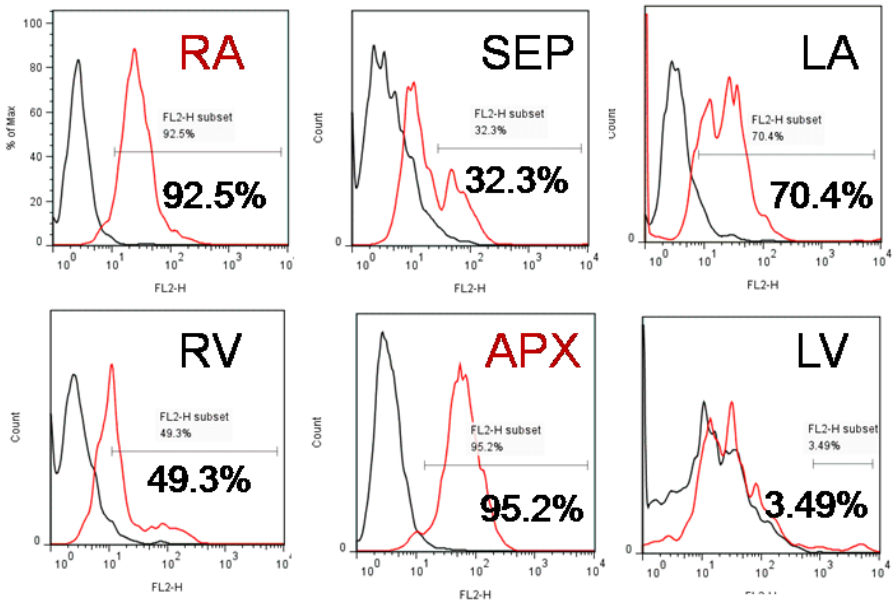

Figure 3-6 FACS analysis for LPAR4 expression results in heart 4 chamber including septum and apex

(A) Mice heart was split into 6 sites of right atrium (RA), left atrium (LA), right ventricle (52), left ventricle (28), septum (SEP) and apex (APX) to evaluate the place for more phase-bright cell generation. In the majority of the right atrium and apex, more phase-bright cells were generated and they had more LPAR4 expression (more than 90%) than any other sites.

A

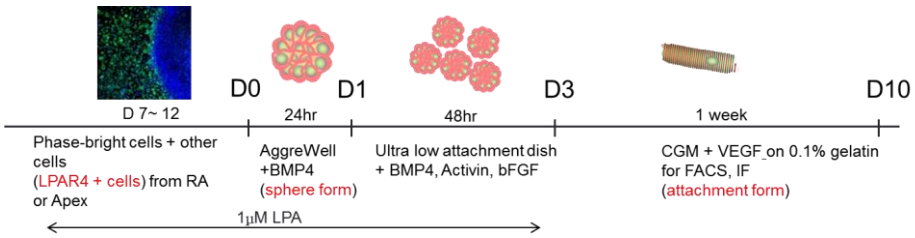

B

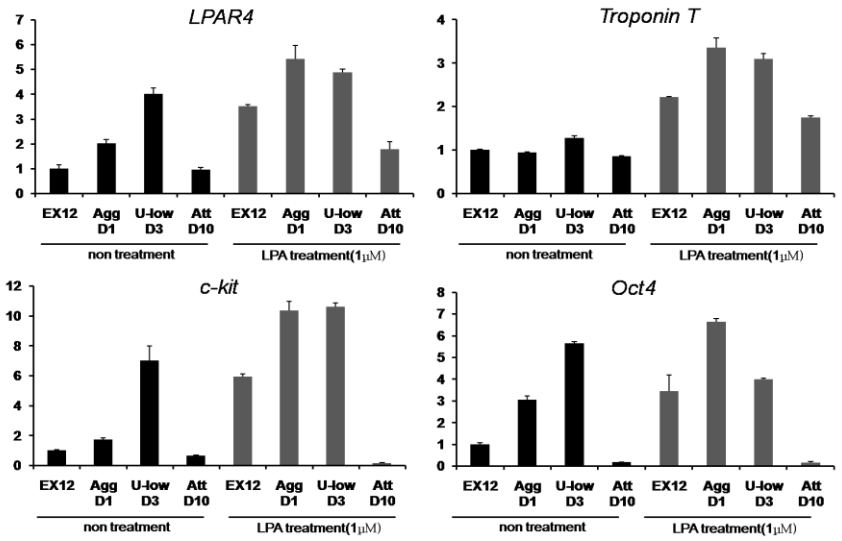

Figure 3-7 Strategy of cardiomyocyte differentiation from phase-bright cell applying 3-dimension form, LPA treatment

(A) Scheme for cardiomyocyte differentiation

(B) Real-time PCR result in each step: Following 3D formation and LPA treatment, LPAR4 gene was increased with Oct4. But after cell attachment to differentiation into cardiomyocyte, stemness genes were rapidly down-regulated while troponin T gene was beginning to increase.

(C)Immune fluorescent staining (red color: troponin-t, blue color: nuclear count staining) and result graph of cell counting Bar: 50 μm

(D)Quantitative analysis by FACS

C

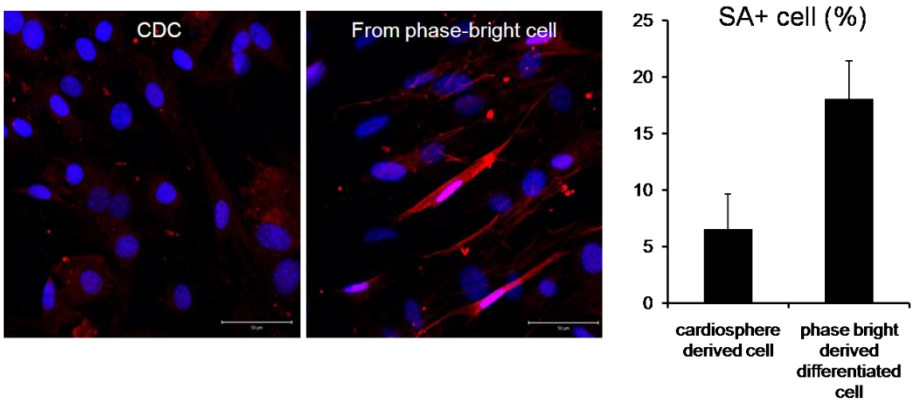

D

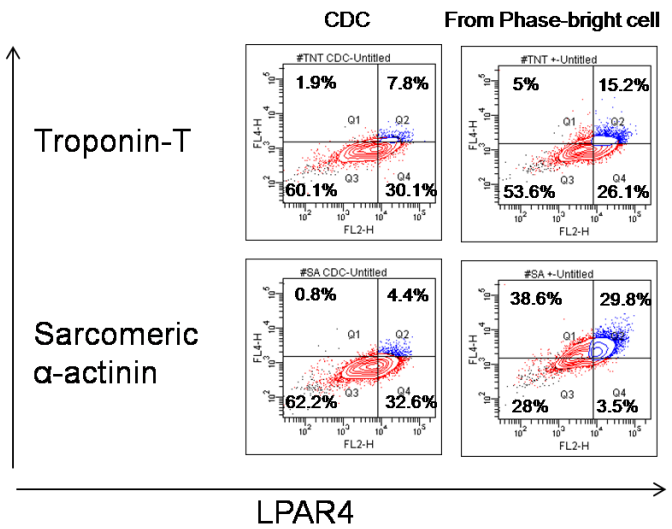

A

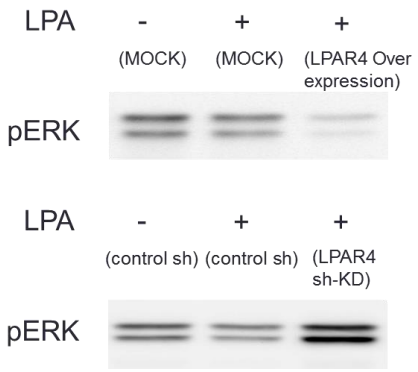

B

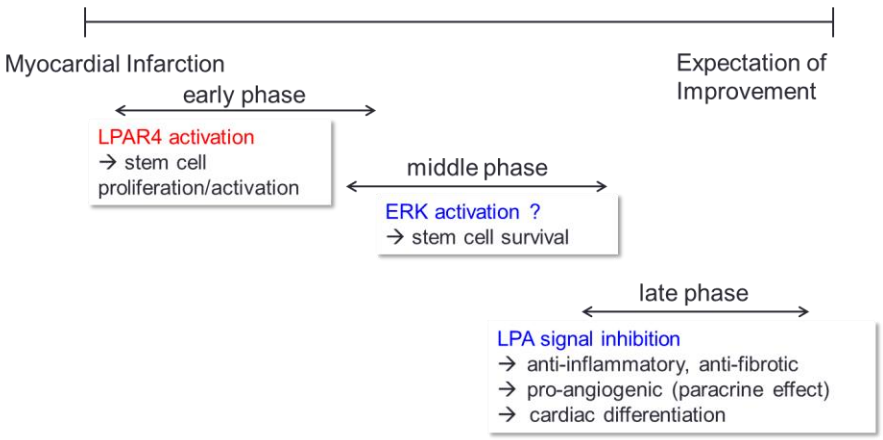

Figure 3-8 Relationship of LPAR4, pERK and suggested future therapeutic strategy to treat myocardial infarction

(A) Western blot result shows pERK was down-regulated under situation of LPAR4 over-expression. On the other hand, knock down of LPAR4 upregulated pERK.

(B) The suggested future therapeutic strategy scheme is illustrated

DISCUSSION

Secondary cardiospheres overcame the huddle: an insufficient cell number of primary cardiospheres and a loss of a stemness propensity of CDC. In fact, a secondary cardiosphere or CDC was easy to handle when subculture (10) but as time goes, primary culture could not be avoided due to loss of pluripotency. It is important to extract complete resident cardiac stem cells without disturbing any other properties. To do that, massive production of cardiac progenitors is necessary in a rapid and a less timely manner in a primary culture status. A primary cardiosphere seems to meet the above mentioned conditions (6); however, only a small number can be gained due to a limited number of phase-bright cells. To extend cardiosphere study, it seemed crucial to obtain a lot of phase-bright cells that retain pluripotency. Before studying phase-bright cells, I put the microarray gene screening data as a reference to find up regulated genes when iPS cells are under a differentiation condition to cardiomyocytes. 110 genes were 2 fold up regulated but I focused on Lysophosphatidic acid receptor4 (LPAR4) gene, one of the G-protein coupled receptors (9). Because the LPAR4+ cell can be easily sorted due to its

membrane localization and also the receptor properties allow downstream signaling studies in the future. LPAR4 is identified as the fourth novel receptor of LPA receptor series and LPAR4 can also respond to its ligand, Lysophosphatidic acid (LPA), depending on its concentration (40). Moreover, during an embryo development, LPAR4 is highly expressed in heart (40-42). Interestingly, I found that a majority of phase-bright cells were LPAR4 positive. When LPA (LPAR4 ligand) was treated to explant tissue, phase-bright-cells were increasingly generated. In this dissertation, I proposed experimental methods to augment number of phase-bright cells produced, increase the stemness capacity by three dimensional cultures together with LPA treatment, and lastly establishing a distinct differentiation stage to cardiomyocytes. More experiments need to be performed to elucidate how LPAR4 is functionally related to increased stemness-related genes observed. I found that ERK activation can be modulated by LPAR4 in both gain- and loss of function of LPAR4 study (Figure 3-8A). In chapter 2, I showed that *Oct4* gene expression level was increased when ERK signaling was blocked. LPA receptor belongs to a family of G protein coupled receptor. It is known that G protein subunits

including Gi/o, Gq, Gs, and G12/13 are known to bind to LPA receptor (53). There has been a report that ERK activation is on the downstream of Gi/o signaling pathway and its upstream molecule is LPA receptor 1 (LPAR1) (41, 53). However, LPAR4 is known to not bind to Gi/o in a neuronal cell-line (41). Based on these facts, it could be suggested that ERK signaling is not directly regulated by LPAR4 but dependent on a situation when the amount of LPAR4 is predominant over LPAR1. In such, there is a less probability for LPA to bind to LPAR1, leading to inhibition of phosphorylation of ERK and its signaling pathway. In the early stage of the development of cardiac diseases, inhibition of ERK by LPAR4 activation may be important for increased production of stemness-related factors and proliferation and activation of stem/progenitor cells. However, ERK activation can be required for the survival of these stem cells in a harsh condition including cardiac diseases (54, 55). Nevertheless, a prolonged activation of this signaling axis could lead to induction of fibrosis which can exacerbate cardiac diseases (47, 56, 57). Therefore, meticulous planning and precise balancing of LPA/LPAR/ERK modulation must be considered for the prevention and treatment of ischemic heart

diseases for future therapy. In conclusion, the finding of LPAR4 expression in heart seems to convey a message that LPAR4 is indeed associated with the activation of cardiac progenitor cells for the differentiation into cardiomyocytes.

REFERENCES

1. Chavakis E, Koyanagi M, Dimmeler S. Enhancing the outcome of cell therapy for cardiac repair: progress from bench to bedside and back. Circulation. 2010;121(2):325-35.
2. Murry CE, Reinecke H, Pabon LM. Regeneration gaps: observations on stem cells and cardiac repair. J Am Coll Cardiol. 2006;47(9):1777-85.
3. Lipinski MJ, Biondi-Zoccai GG, Abbate A, Khianey R, Sheiban I, Bartunek J, et al. Impact of intracoronary cell therapy on left ventricular function in the setting of acute myocardial infarction: a collaborative systematic review and meta-analysis of controlled clinical trials. J Am Coll Cardiol. 2007;50(18):1761-7.
4. Abdel-Latif A, Bolli R, Tleyjeh IM, Montori VM, Perin EC, Hornung CA, et al. Adult bone marrow-derived cells for cardiac repair: a systematic review and meta-analysis. Arch Intern Med. 2007;167(10):989-97.
5. Bolli R, Chugh AR, D'Amario D, Loughran JH, Stoddard MF, Ikram S, et al. Cardiac stem cells in patients with ischaemic cardiomyopathy (SCIPIO): initial results of a randomised phase 1 trial. Lancet. 2011;378(9806):1847-57.
6. Messina E, De Angelis L, Frati G, Morrone S, Chimenti S, Fiordaliso F, et al. Isolation and expansion of adult cardiac stem cells from human and murine heart. Circ Res. 2004;95(9):911-21.
7. Beltrami AP, Barlucchi L, Torella D, Baker M, Limana F, Chimenti S, et al. Adult cardiac stem cells are multipotent and support myocardial regeneration. Cell. 2003;114(6):763-76.
8. Pfister O, Mouquet F, Jain M, Summer R, Helmes M, Fine A, et al. CD31- but Not CD31+ cardiac side population cells exhibit functional cardiomyogenic differentiation. Circ Res. 2005;97(1):52-61.
9. Noguchi K, Ishii S, Shimizu T. Identification of p2y9/GPR23 as a novel G protein-coupled receptor for lysophosphatidic acid, structurally distant from the Edg family. J Biol Chem. 2003;278(28):25600-6.
10. Smith RR, Barile L, Cho HC, Leppo MK, Hare JM, Messina E, et al. Regenerative potential of cardiosphere-derived cells expanded from percutaneous endomyocardial biopsy specimens. Circulation. 2007;115(7):896-908.
11. Oh IY, Yoon CH, Hur J, Kim JH, Kim TY, Lee CS, et al. Involvement of E-selectin in recruitment of endothelial progenitor cells and angiogenesis in ischemic muscle. Blood. 2007;110(12):3891-9.
12. Dani C, Smith AG, Dessolin S, Leroy P, Staccini L, Villageois P, et al. Differentiation of embryonic stem cells into adipocytes in vitro. J Cell Sci. 1997;110 (Pt 11):1279-85.
13. Dang SM, Kyba M, Perlingeiro R, Daley GQ, Zandstra PW.

Efficiency of embryoid body formation and hematopoietic development from embryonic stem cells in different culture systems. Biotechnol Bioeng. 2002;78(4):442-53.
14. Yoon CH, Koyanagi M, Iekushi K, Seeger F, Urbich C, Zeiher AM, et al. Mechanism of improved cardiac function after bone marrow mononuclear cell therapy: role of cardiovascular lineage commitment. Circulation. 2010;121(18):2001-11.
15. Koyanagi M, Iwasaki M, Rupp S, Tedesco FS, Yoon CH, Boeckel JN, et al. Sox2 transduction enhances cardiovascular repair capacity of blood-derived mesoangioblasts. Circ Res. 2010;106(7):1290-302.
16. Scherr M, Battmer K, Blomer U, Schiedlmeier B, Ganser A, Grez M, et al. Lentiviral gene transfer into peripheral blood-derived CD34+ NOD/SCID-repopulating cells. Blood. 2002;99(2):709-12.
17. Chang SA, Lee EJ, Kang HJ, Zhang SY, Kim JH, Li L, et al. Impact of myocardial infarct proteins and oscillating pressure on the differentiation of mesenchymal stem cells: effect of acute myocardial infarction on stem cell differentiation. Stem Cells. 2008;26(7):1901-12.
18. Hahn JY, Cho HJ, Bae JW, Yuk HS, Kim KI, Park KW, et al. Beta-catenin overexpression reduces myocardial infarct size through differential effects on cardiomyocytes and cardiac fibroblasts. J Biol Chem. 2006;281(41):30979-89.
19. Cho HJ, Lee N, Lee JY, Choi YJ, Ii M, Wecker A, et al. Role of host tissues for sustained humoral effects after endothelial progenitor cell transplantation into the ischemic heart. J Exp Med. 2007;204(13):3257-69.
20. Terrovitis JV, Smith RR, Marban E. Assessment and optimization of cell engraftment after transplantation into the heart. Circ Res. 2010;106(3):479-94.
21. Galli R, Gritti A, Bonfanti L, Vescovi AL. Neural stem cells: an overview. Circ Res. 2003;92(6):598-608.
22. Rietze RL, Valcanis H, Brooker GF, Thomas T, Voss AK, Bartlett PF. Purification of a pluripotent neural stem cell from the adult mouse brain. Nature. 2001;412(6848):736-9.
23. Ma BF, Liu XM, Xie XM, Zhang AX, Zhang JQ, Yu WH, et al. Slower cycling of nestin-positive cells in neurosphere culture. Neuroreport. 2006;17(4):377-81.
24. Lee EJ, Park SJ, Kang SK, Kim GH, Kang HJ, Lee SW, et al. Spherical bullet formation via E-cadherin promotes therapeutic potency of mesenchymal stem cells derived from human umbilical cord blood for myocardial infarction. Mol Ther. 2012;20(7):1424-33.
25. Favata MF, Horiuchi KY, Manos EJ, Daulerio AJ, Stradley DA, Feeser WS, et al. Identification of a novel inhibitor of mitogen-activated protein kinase kinase. J Biol Chem. 1998;273(29):18623-32.
26. Vlahos CJ, Matter WF, Hui KY, Brown RF. A specific inhibitor of phosphatidylinositol 3-kinase, 2-(4-morpholinyl)-8-phenyl-4H-1-

benzopyran-4-one (LY294002). J Biol Chem. 1994;269(7):5241-8.
27. Peerani R, Zandstra PW. Enabling stem cell therapies through synthetic stem cell-niche engineering. J Clin Invest. 2010;120(1):60-70.
28. Campos LS, Leone DP, Relvas JB, Brakebusch C, Fassler R, Suter U, et al. Beta1 integrins activate a MAPK signalling pathway in neural stem cells that contributes to their maintenance. Development. 2004;131(14):3433-44.
29. Ishii S, Okada Y, Kadoya T, Matsuzaki Y, Shimazaki T, Okano H. Stromal cell-secreted factors promote the survival of embryonic stem cell-derived early neural stem/progenitor cells via the activation of MAPK and PI3K-Akt pathways. J Neurosci Res. 2010;88(4):722-34.
30. Curry JM, Eubank TD, Roberts RD, Wang Y, Pore N, Maity A, et al. M-CSF signals through the MAPK/ERK pathway via Sp1 to induce VEGF production and induces angiogenesis in vivo. PLoS One. 2008;3(10):e3405.
31. Ryuto M, Ono M, Izumi H, Yoshida S, Weich HA, Kohno K, et al. Induction of vascular endothelial growth factor by tumor necrosis factor alpha in human glioma cells. Possible roles of SP-1. J Biol Chem. 1996;271(45):28220-8.
32. Marshall CJ. Specificity of receptor tyrosine kinase signaling: transient versus sustained extracellular signal-regulated kinase activation. Cell. 1995;80(2):179-85.
33. von Kriegsheim A, Baiocchi D, Birtwistle M, Sumpton D, Bienvenut W, Morrice N, et al. Cell fate decisions are specified by the dynamic ERK interactome. Nat Cell Biol. 2009;11(12):1458-64.
34. Williams AR, Hatzistergos KE, Addicott B, McCall F, Carvalho D, Suncion V, et al. Enhanced effect of combining human cardiac stem cells and bone marrow mesenchymal stem cells to reduce infarct size and to restore cardiac function after myocardial infarction. Circulation. 2013;127(2):213-23.
35. Laflamme MA, Murry CE. Heart regeneration. Nature. 2011;473(7347):326-35.
36. Leri A, Anversa P. Stem cells: bone-marrow-derived cells and heart failure--the debate goes on. Nat Rev Cardiol. 2013;10(7):372-3.
37. Strauer BE, Steinhoff G. 10 years of intracoronary and intramyocardial bone marrow stem cell therapy of the heart: from the methodological origin to clinical practice. J Am Coll Cardiol. 2011;58(11):1095-104.
38. Jeevanantham V, Butler M, Saad A, Abdel-Latif A, Zuba-Surma EK, Dawn B. Adult bone marrow cell therapy improves survival and induces long-term improvement in cardiac parameters: a systematic review and meta-analysis. Circulation. 2012;126(5):551-68.
39. Sumida H, Noguchi K, Kihara Y, Abe M, Yanagida K, Hamano F, et al. LPA4 regulates blood and lymphatic vessel formation during mouse embryogenesis. Blood. 2010;116(23):5060-70.
40. Lee Z, Cheng CT, Zhang H, Subler MA, Wu J, Mukherjee A, et

al. Role of LPA4/p2y9/GPR23 in negative regulation of cell motility. Mol Biol Cell. 2008;19(12):5435-45.
41. Yanagida K, Ishii S, Hamano F, Noguchi K, Shimizu T. LPA4/p2y9/GPR23 mediates rho-dependent morphological changes in a rat neuronal cell line. J Biol Chem. 2007;282(8):5814-24.
42. Wang F, Hou J, Han B, Nie Y, Cong X, Hu S, et al. Developmental changes in lysophospholipid receptor expression in rodent heart from near-term fetus to adult. Mol Biol Rep. 2012;39(9):9075-84.
43. Hausmann J, Kamtekar S, Christodoulou E, Day JE, Wu T, Fulkerson Z, et al. Structural basis of substrate discrimination and integrin binding by autotaxin. Nature structural & molecular biology. 2011;18(2):198-204.
44. Tanaka M, Okudaira S, Kishi Y, Ohkawa R, Iseki S, Ota M, et al. Autotaxin stabilizes blood vessels and is required for embryonic vasculature by producing lysophosphatidic acid. J Biol Chem. 2006;281(35):25822-30.
45. Dusaulcy R, Rancoule C, Gres S, Wanecq E, Colom A, Guigne C, et al. Adipose-specific disruption of autotaxin enhances nutritional fattening and reduces plasma lysophosphatidic acid. Journal of lipid research. 2011;52(6):1247-55.
46. Hama K, Aoki J, Fukaya M, Kishi Y, Sakai T, Suzuki R, et al. Lysophosphatidic acid and autotaxin stimulate cell motility of neoplastic and non-neoplastic cells through LPA1. J Biol Chem. 2004;279(17):17634-9.
47. Rancoule C, Viaud M, Gres S, Viguerie N, Decaunes P, Bouloumie A, et al. Pro-fibrotic activity of lysophosphatidic acid in adipose tissue: in vivo and in vitro evidence. Biochim Biophys Acta. 2014;1841(1):88-96.
48. Pradere JP, Gonzalez J, Klein J, Valet P, Gres S, Salant D, et al. Lysophosphatidic acid and renal fibrosis. Biochim Biophys Acta. 2008;1781(9):582-7.
49. Tager AM, LaCamera P, Shea BS, Campanella GS, Selman M, Zhao Z, et al. The lysophosphatidic acid receptor LPA1 links pulmonary fibrosis to lung injury by mediating fibroblast recruitment and vascular leak. Nat Med. 2008;14(1):45-54.
50. Lee SJ, Chan TH, Chen TC, Liao BK, Hwang PP, Lee H. LPA1 is essential for lymphatic vessel development in zebrafish. FASEB journal : official publication of the Federation of American Societies for Experimental Biology. 2008;22(10):3706-15.
51. Ishii I, Fukushima N, Ye X, Chun J. Lysophospholipid receptors: signaling and biology. Annual review of biochemistry. 2004;73:321-54.
52. Yamahara K, Fukushima S, Coppen SR, Felkin LE, Varela-Carver A, Barton PJ, et al. Heterogeneic nature of adult cardiac side population cells. Biochem Biophys Res Commun. 2008;371(4):615-20.
53. Gardell SE, Dubin AE, Chun J. Emerging medicinal roles for

lysophospholipid signaling. Trends in molecular medicine. 2006;12(2):65-75.
54. Chen J, Baydoun AR, Xu R, Deng L, Liu X, Zhu W, et al. Lysophosphatidic acid protects mesenchymal stem cells against hypoxia and serum deprivation-induced apoptosis. Stem Cells. 2008;26(1):135-45.
55. Tao R, Hoover HE, Zhang J, Honbo N, Alano CC, Karliner JS. Cardiomyocyte S1P1 receptor-mediated extracellular signal-related kinase signaling and desensitization. Journal of cardiovascular pharmacology. 2009;53(6):486-94.
56. Aoki J, Inoue A, Okudaira S. Two pathways for lysophosphatidic acid production. Biochim Biophys Acta. 2008;1781(9):513-8.
57. Smyth SS, Mueller P, Yang F, Brandon JA, Morris AJ. Arguing the case for the autotaxin-lysophosphatidic acid-lipid phosphate phosphatase 3-signaling nexus in the development and complications of atherosclerosis. Arterioscler Thromb Vasc Biol. 2014;34(3):479-86.

국문 초록

심장 내에서 존재하고 있는 성체 심장줄기세포는 극 미량으로 존재한다. 세포 치료를 위해서는 충분한 양을 확보하는 것이 중요한데, 부족한 양을 극복하고자 cardiosphere-derived cell (CDC)이 소개되었다. 그러나 2 차원 배양법으로 확보된 CDC 는 3 차원 배양 상태였던 Cardiosphere 보다 낮은 줄기세포 성을 보이기 때문에, 이 CDC 를 다시 sphere 형태로 배양함으로써 회복할 수 있었다. 이런 노력에도 불구하고 계대배양을 거치면서 줄기세포 성이 점차 감소하여 동물의 희생과 환자의 생검시료를 확보를 동반한 초대배양을 재 실시 해야 하는 부담은 여전히 남아있다. 본 박사학위 논문에는 발명한 심장 내 성체줄기세포의 3 차원 배양법과 새롭게 발견한 몇 가지 사실들을 기술하였다. 그리고 조직배양과 3 차원배양법을 적용하여 심장전구세포라고 생각되는 phase-bright cell 을 많이 증대시킬 수 있는 새로운 전략을 설명하고자 한다.

마이크로 어레이 분석을 통한 결과 LPA 수용체 4 (LPAR4)가 Phase-bright cell 에서 강하게 발현하는 것을 알게 되었다. 배위자인 LPA 를 처리했을 때 phase-bright cell 의 빠른 증식과 LPAR4 유전자 발현이 3 배 이상 증가하였다. LPA 처리와 함께 3 차원으로 배양된 Phase-bright cell 은 LPAR4 뿐 아니라 줄기세포성에 관련된 유전자인 Oct4, c-kit 도 같이 증가하였다. LPAR4 양성 phase-

bright cell 을 심근세포로 분화시킨 결과 CDC 로 분화시킨 것 보다 심근세포의 특이 인자인 Troponin-T, sarcomeric α-actinin 이 더 많이 증가하는 것을 유세포 분석을 통해 검증했다. 아울러 LPAR4 와 stemness 와 상관관계를 제시하여 앞으로의 허 혈성 심장 질병의 치료전략을 토의부분에 제시하였다. 끝으로, 심장 내에서 LPAR4 의 발현은 심근세포로 분화하기 위한 심근전구세포의 활성에 중요한 메시지를 담고 있다고 본다.

주요어: 심혈관질환, 세포치료제, 성체줄기세포, 카디오스피어

학 번: 2008-22012